

Keratoconus Indices Indicative of Progression using the Pentacam HR®

A bachelor thesis
to the University of Applied Sciences, Aalen, Germany
in fulfillment of the
thesis requirement for the degree of

Bachelor of Science

Augenoptik und Hörakustik/Augenoptik

by

Dorothee Bandle

12.12.2019

First Reviewer: Prof. Dr. Anna Nagl, Dipl.-Ing. (FH) Ralf Michels

Second Reviewer: Dr. Luigina Sorbara (OD, MSc, FAAO, FBCLA, Diplo)

Declaration of Authorship

I hereby declare that the thesis submitted is my own unaided work. All direct or indirect sources used are acknowledged as references. I am aware that the thesis in digital form can be examined for the use of unauthorized aid and in order to determine whether the thesis as a whole or parts incorporated in it may be deemed as plagiarism. For the comparison of my work with existing sources I agree that it shall be entered in a database where it shall also remain after examination, to enable comparison with future theses submitted. Further rights of reproduction and usage, however, are not granted here.

This paper was not previously presented to another examination board and has not been published.

Ehrenwörtliche Erklärung

Ich erkläre hiermit ehrenwörtlich, dass ich die vorliegende Arbeit selbständig angefertigt habe. Die aus fremden Quellen direkt und indirekt übernommenen Gedanken sind als solche kenntlich gemacht. Ich weiß, dass die Arbeit in digitalisierter Form daraufhin überprüft werden kann, ob unerlaubte Hilfsmittel verwendet wurden und ob es sich – insgesamt oder in Teilen – um ein Plagiat handelt. Zum Vergleich meiner Arbeit mit existierenden Quellen darf sie in eine Datenbank eingestellt werden und nach der Überprüfung zum Vergleich mit künftig eingehenden Arbeiten dort verbleiben. Weitere Vervielfältigungs- und Verwertungsrechte werden dadurch nicht eingeräumt.

Die Arbeit wurde weder einer anderen Prüfungsbehörde vorgelegt noch veröffentlicht.

Kirchheim/Teck, den 12.12.2019

.....

Abstract

Purpose: To determine the indices of the Pentacam HR® which change enough in longitudinal data to detect and predict Keratoconus progression and how they correlate to demographic/other predictor variables.

Methods: In this retrospective chart review topographic, tomographic and elevation data from 134 subjects with two visits were collected from the Pentacam HR®. The subjects were divided into two groups as diagnosed with Keratoconus and normal eyes. The Keratoconus group was subdivided into cross linked and not cross linked eyes and whether or not they had atopic disease or not. The parameters were compared for each of the groups and between the two visits for each group.

Results: The normal eyes were significantly different compared to the keratoconic eyes in almost all factors and indices (all $p > 0.05$). Comparing the CXL and non CXL group only the density was found to be significantly higher in the CXL group ($p < 0.05$). In the Non CXL group comparing the two visits K flat steepened significantly ($p = 0.021$), the pachymetry of the thinnest point increased ($p = 0.02$) and Dt was reduced ($p = 0.027$). Within the CXL group K steep steepened ($p = 0.028$), CKI increased ($p = 0.046$) and the location of the thinnest point changed ($p = 0.024$). IHD increased for the Non CXL, CXL groups and the atopic, Non atopic groups (all $p < 0.05$). There were no differences found in any of the indices or factors when comparing the atopic to the non atopic groups at each visit ($p > 0.05$).

Conclusion: In conclusion, this review on a limited number of KC participants has demonstrated that the Pentacam HR® and its factors and indices can be useful in detecting the progression of KC with and without CXL and atopic disease, in addition, to their use in early diagnosis of KC when compare to controls.

Zusammenfassung

Ziel: Bestimmung der Indizes der Pentacam HR®, die sich über längere Zeit stark genug ändern, um Keratokonusprogression zu erkennen und vorherzusagen und wie diese Indizes mit demografischen und anderen Variablen korrelieren.

Methoden: In dieser retrospektiven Übersicht wurden topografische, tomografische und Höhendaten von 134 Probanden mit zwei Messungen der Pentacam HR® gesammelt. Die Probanden wurden in zwei Gruppen eingeteilt, Augen bei denen Keratokonus diagnostiziert wurden und normale Augen. Die Keratokonus-Gruppe wurde in weitere Gruppen unterteilt, je nachdem ob Crosslinking durchgeführt wurde oder nicht und ob die Probanden eine atopische Erkrankung hatten oder nicht. Die Parameter wurden zwischen den Gruppen und zwischen den beiden Besuchen für jede Gruppe verglichen.

Ergebnisse: Die normalen Augen unterschieden sich in fast allen Faktoren und Indizes signifikant von den keratokonischen Augen (alle $p > 0,05$). Beim Vergleich der CXL- und der Nicht-CXL-Gruppe wurde festgestellt, dass nur die Hornhautdicke in der CXL-Gruppe signifikant höher war ($p < 0,05$). Beim Vergleich der beiden Messungen der Nicht-CXL Gruppe zeigte sich, dass K flach signifikant steiler wurde ($p = 0,021$), die Pachymetrie der dünnsten Stelle signifikant zunahm ($p = 0,02$) und sich Dt verringerte ($p = 0,027$). Innerhalb der CXL-Gruppe wurde K steil signifikant steiler ($p = 0,028$), CKI stieg an ($p = 0,046$) und die Position der dünnsten Stelle änderte sich ($p = 0,024$). Sowohl in der Nicht-CXL- und der CXL-Gruppe als auch in den Gruppen mit und ohne atopische Erkrankung erhöhte sich der IHD signifikant (alle $p < 0,05$). Beim Vergleich der atopischen und der nicht atopischen Gruppe wurde weder in der ersten noch in der zweiten Messung ein signifikanter Unterschied der Indizes oder Faktoren festgestellt ($p > 0,05$).

Schlussfolgerung: Zusammenfassend hat diese Überprüfung einer begrenzten Anzahl an Probanden gezeigt, dass die Faktoren und Indizes der Pentacam HR®, zusätzlich zu ihrer Anwendung zur frühen Diagnose von KC, hilfreich zur Erkennung der Keratokonusprogression mit und ohne CXL und atopischen Erkrankungen sein können.

Acknowledgements

First of all, I would like to thank Dr. Luigina Sorbara for her support and encouragement in the last months, for her help with the language and her enormous knowledge. Thanks to her I had a great time in Waterloo and learnt a lot.

Next, I would like to thank Prof. Dr. Anna Nagl. Without her it would not have been possible to write my Bachelor thesis in cooperation with the University of Waterloo.

I would like to thank the School of Optometry and Vision Science in Waterloo for the opportunity to come to Canada as a Visiting Researcher.

Finally, I would like to thank Dipl.-Ing. (FH) Ralf Michels for his help in all my organizational questions.

Table of Content

Declaration of Authorship	II
Abstract	III
Zusammenfassung.....	IV
Acknowledgements	V
List of Figures.....	VIII
List of Tables	IX
1 Introduction	1
1.1 Corneal Shape	1
1.2 Change in Corneal Shape	2
1.2.1 Keratoconus	2
1.2.2 Aberrations with KC	8
1.2.3 Management of KC and Corneal Cross linking.....	9
1.2.4 Other corneal disorders	10
2 Measurement of Corneal Shape	11
2.1 Topography	11
2.2 Tomography	12
2.3 Advantages of Pentacam HR®	15
3 The Study.....	23
3.1 Purpose and Motivation.....	23
3.2 Objectives	23
3.3 Hypothesis	23

3.4	Study design	24
3.5	Participants	24
3.5.1	Sample size calculation	24
3.5.2	Number of participants.....	24
3.5.3	Inclusion and exclusion criteria	25
3.6	Statistical Analysis.....	25
3.7	Results Part I.....	26
3.7.1	Demographic	26
3.7.2	Leading and lagging eye.....	27
3.7.3	Influence of systemic disease	28
3.7.4	Comparing Normal to Non CXL to CXL	31
3.8	Results Part II (Non CXL vs. CXL)	36
3.8.1	Curvature data	36
3.8.2	Elevation data	36
3.8.3	Pachymetry data.....	37
3.8.4	Aberrations	37
3.8.5	Densitometry.....	38
3.8.6	Final D value and TKC.....	39
3.9	Results Part III (comparing visits by CXL)	39
3.9.1	Curvature data	39
3.9.2	Elevation data	40
3.9.3	Pachymetry data.....	42

3.9.4	Aberrations	43
3.9.5	Densitometry.....	43
3.9.6	Final D value and TKC.....	44
3.10	Discussion.....	45
3.11	Conclusion	47
4	Literature Cited.....	VIII

List of Figures

Figure 1-1	Anatomy and physiology of the cornea by DelMonte et al (13)	2
Figure 1-2	Keratoconus profiles (picture courtesy of L. Sorbara)	3
Figure 1-3	Oxidative Stress (picture courtesy of L. Sorbara).....	4
Figure 1-4	Morphological changes in all corneal layers by Sherwin et al (37)	7
Figure 2-1	Placido disc (picture courtesy of L. Sorbara).....	12
Figure 2-2	Orbscan II (picture courtesy of L. Sorbara)	13
Figure 2-3	Orbscan Pachymetry map (picture courtesy of L. Sorbara)	13
Figure 2-4	Pentacam HR® (picture courtesy of L. Sorbara).....	14
Figure 2-5	Pentacam HR®: 4 Maps display (picture courtesy of L. Sorbara)	15
Figure 2-6	Scheimpflug image density (picture courtesy of L. Sorbara)	16
Figure 2-7	BAD display elevation data (picture courtesy of L. Sorbara)	20
Figure 2-8	BAD display pachymetry data (picture courtesy of L. Sorbara)	21
Figure 3-1	Densitometry Non CXL vs. CXL Visit 1 vs. Visit 2	38
Figure 3-2	K values Non CXL vs. CXL Visit 1 vs. Visit 2	40

Figure 3-3 IHD Non CXL vs. CXL Visit 1 vs. Visit 2	41
--	----

List of Tables

Table 1-1 High-risk characteristics for progression of Keratoconus by Shetty et al (36)	5
Table 2-1 Amsler-Krumeich classification (adapted from Krumeich et al (83))	18
Table 2-2 Limiting values for topographic indices (adapted from the Pentacam User Manual (79))	19
Table 2-3 ABCD grading system adapted by Belin et al. (85) (anterior and posterior radius of curvature (ARC. PRC), best corrected distance visual acuity (BDVA)).....	22
Table 3-1 Demographics of CXL and Non CXL.....	26
Table 3-2 Mean time difference between visits for CXL and Non CXL.....	26
Table 3-3 Demographics Control, Non CXL and CXL	27
Table 3-4 Mean time difference between V1 and V2 T-Test	27
Table 3-5 Comparing leading eye and lagging eye	28
Table 3-6 Demographics of participants with and without atopic disease	28
Table 3-7 With (Group 1) and Without (Group 2) atopic disease Visit 1	29
Table 3-8 With (Group 1) and without (Group 2) atopic disease Visit 2.....	30
Table 3-9 Normal compared to Non CXL Visit 1.....	31
Table 3-10 Normal compared to Non CXL Visit 2.....	32
Table 3-11 Normal compared to CXL Visit 1	33
Table 3-12 Normal compared to CXL Visit 2	34
Table 3-13 Normal V1 compared to V2	35

Table 3-14 Curvature data Non CXL vs. CXL at each visit.....	36
Table 3-15 Elevation data Non CXL vs. CXL at each visit.....	36
Table 3-16 Pachymetry data Non CXL vs. CXL at each visit	37
Table 3-17 Aberrations Non CXL vs. CXL at each visit	37
Table 3-18 Density Non CXL vs. CXL at each visit	38
Table 3-19 D and TKC Non CXL vs. CXL at each visit.....	39
Table 3-20 Curvature data Non CXL comparing each visit	39
Table 3-21 Curvature data CXL comparing each visit	40
Table 3-22 Elevation data Non CXL comparing visits	41
Table 3-23 Elevation data CXL comparing visits	41
Table 3-24 Pachymetry data Non CXL comparing visits	42
Table 3-25 Pachymetry data CXL comparing visits	42
Table 3-26 Aberrations Non CXL comparing visits.....	43
Table 3-27 Aberrations CXL comparing visits	43
Table 3-28 Density Non CXL comparing visits	43
Table 3-29 Density CXL comparing visits.....	44
Table 3-30 D and TKC Non CXL comparing visits	44
Table 3-31 D and TKC CXL comparing visits	44

1 Introduction

1.1 Corneal Shape

The transparent cornea chiefly contributes to the refracting system of the eye and is one of the most important aspects of the eyes. With roughly a radius of curvature of approximately 43.25 (± 1.53) D (1) it is responsible for 66% of the refractive system of the eye. (2) Its average diameter in the normal adult population is 11.71 (± 0.42) mm (3) and the mean front surface central radius is 7.72 (± 0.27) mm and 6.71 (± 0.23) mm for the back surface. (4) The mean total corneal thickness increases centrally from 540 (± 40) μm up to 640 (± 40) μm in the periphery, whereas the mean epithelial thickness remains constant across the entire cornea (approximately 52 (± 3) μm). (5, 6) The shape of the cornea is a prolate ellipse, which means its curvature flattens from the centre to the periphery. (4) This resulting asphericity reduces spherical aberration and improves the retinal imaging. (7) The radius of curvature and the thickness of the cornea show no difference with aging. (8–10) Studies show that from a young age until around 50 years of age that the shape of the cornea is maintained. (11, 12)

The cornea is protected by a multi-layered tear film and consists of five different cellular layers (Figure 1-1). The outer most layer, the epithelium, has a barrier function to the outside environment to stop toxins and microbes from entering the rest of the cornea. (13) It has four to six layers of cells and is 40-50 μm thick. (14) There are three different layers: the superficial cells, the wing cells and the basal cells. (13) The basal cells are capable of mitosis and regenerate quickly. (15) Below the epithelium lies Bowman's membrane. This acellular layer is approximately 15 μm thick, biomechanically stiff and with its help the cornea maintains its shape. When it is injured, it will develop scars. (13) The next layer is the stroma, which comprises 80% to 85% of the thickness of the cornea. (13) It consists of parallel-arranged layers of collagen fibrils. This organization of fibrils leads to the required transparency of the cornea. (16) Keratocytes are quiescent cells in the stroma. After injury, they either undergo apoptosis (programmed cell death) or transform into repair phenotypes. (17)

Beneath the stroma lies Descemet's membrane, which is the basement membrane of the endothelium. Its thickness increases with age from approximately 2 μm to 10 μm . (18)

The innermost layer is the endothelium with just one layer of cells. These cells are not able to regenerate but the remaining cells grow and change their shape to fill the space of degenerated and lost cells. (13)

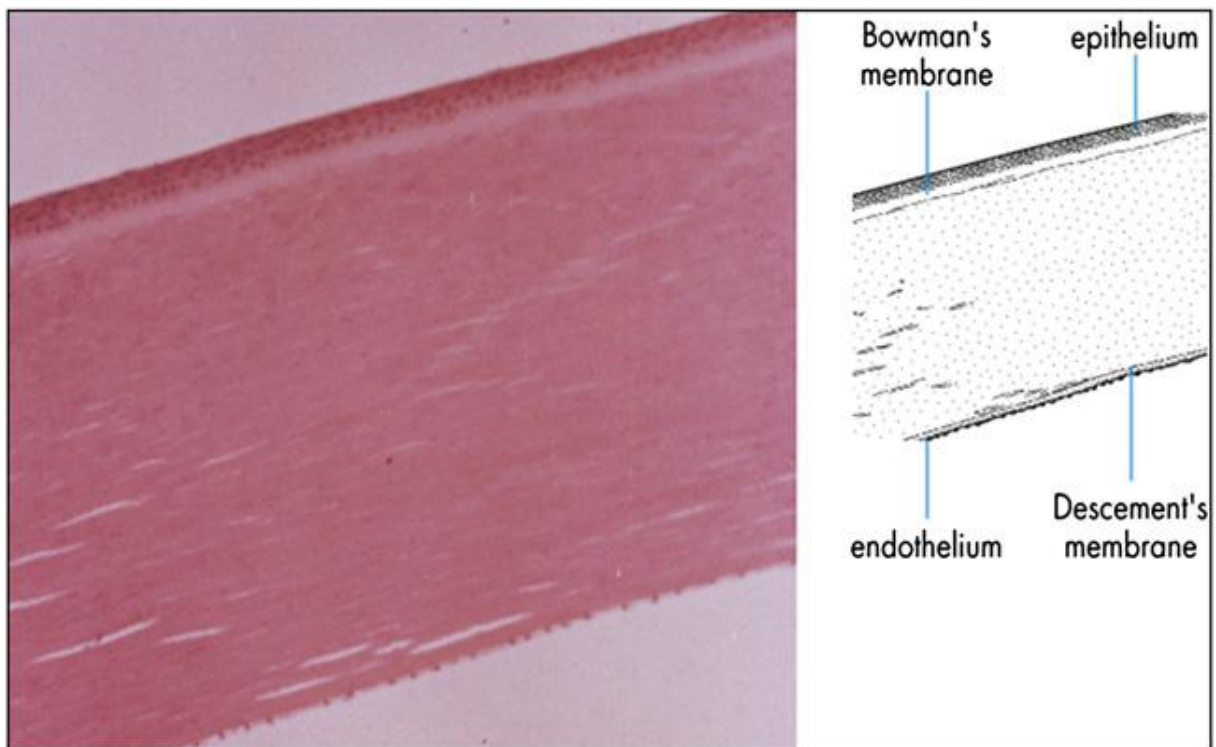


Figure 1-1 Anatomy and physiology of the cornea by DelMonte et al (13)

1.2 Change in Corneal Shape

1.2.1 Keratoconus

In some cases, the cornea does not maintain its regular shape and shows ectasia that is, a bulging forward. Keratoconus (KC) is a degenerative disorder of the cornea that leads to a progressive non-inflammatory cornea thinning. (see Figure 1-2) As a result of this thinning and bulging, which occurs in the posterior cornea first, the protrusion and the conical shape induces irregular astigmatism.

According to Rabinowitz, KC normally begins at puberty and progresses until the age of thirty or forty. (19)

The incidence of KC varies between 50 and 230 per 100,000. (19) Kennedy et al reported a prevalence of 54.5 per 100,000 in Minnesota (20) but it ranges from 0.3 per 100,000 in Russia (21) to 2300 per 100,000 in Central India (22). Two studies found a 4.4-7.5 times higher incidence in Asian populations than in Caucasians. (23, 24) However, the prevalence could be higher as it should be considered that early KC may not be detected or certainly not diagnosed.

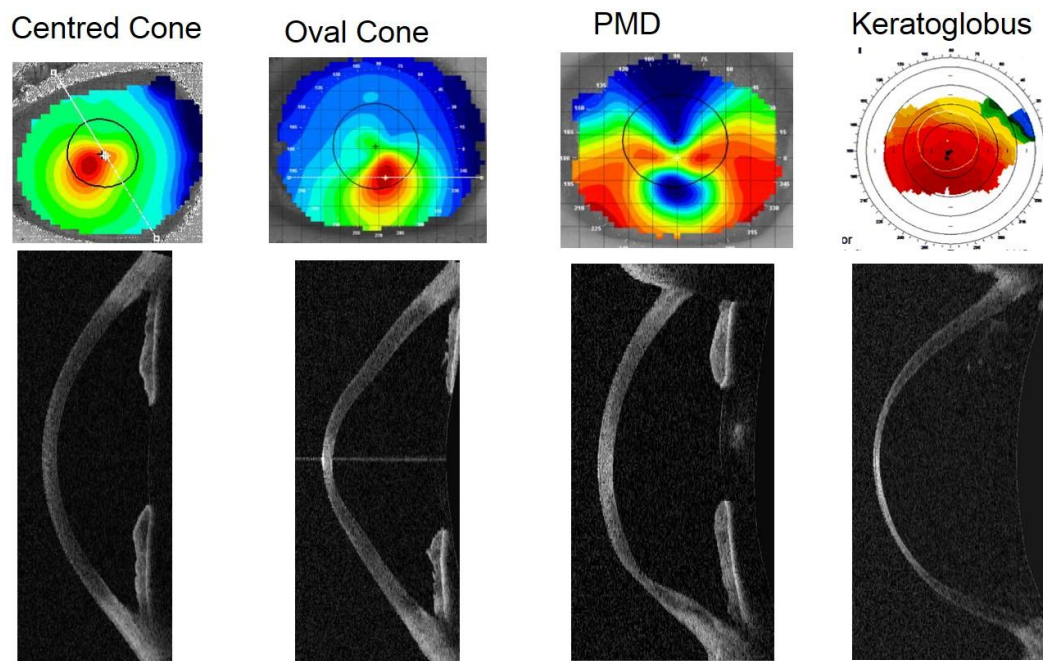


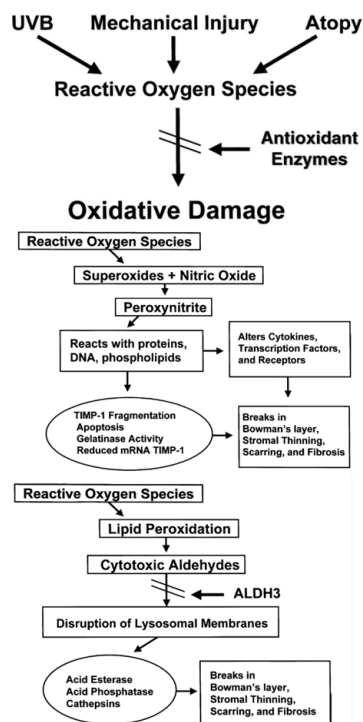
Figure 1-2 Keratoconus profiles (picture courtesy of L. Sorbara)

Pathogenesis of KC

Currently, the pathogenesis of keratoconus is still not completely understood. Gomes et al. have categorized the multitude of pathogenic factors in keratoconus into four major components: genetics, biochemical, biomechanical, and environmental. (25) Genetics may have an influence as 6-10 % of KC patients have a family history of the disease. (26, 27) Further, KC has been associated with connective tissue disorders, Down syndrome, Leber's congenital amaurosis and Marfan syndrome. (19, 28)

External factors such as UV-light, poor contact lens fitting, eye rubbing and allergies lead to oxidative stress. (see Figure 1-3) (29) Keratoconic corneas do not seem to be able to process the oxidative stress as well as normal corneas. (30)

Moreover, atopic diseases such as hay fever and asthma seem to affect and are associated with KC. (31) According to Bawazeer et al. eye rubbing often caused by atopic disease is the most important risk factor. (32) This association has been attributed to an increase in hydrostatic tissue pressure, corneal temperature, and protease activity in the corneal tissue. (33)



Oxidative Stress is an altered balance between ROS and RNS formation and removal causing cytotoxicity and cell damage.

Sources of ↑ROS/RNS include: atopy/allergy, UVB, eye rubbing, inflammation from poor CL fit and other sources

There is an increase in peroxide and superoxide hydroxyl groups (ROS) along with increase in nitric oxide + superoxide = peroxynitrite (RNS).

Increased cytotoxic aldehydes cause mtDNA cell damage which leads to more ROS/RNS production and accumulation (viscous cycle).

Leading to oxidative damage which causes abnormal cell function and increased activation and upregulation of degradative enzymes which leads to corneal thinning.

Atilano and Kenney, Accumulation of Mitochondrial DNA Damage in Keratoconus Corneas. IOVS, 46(4) (2005):1256-63.
Kenney, MC, Brown, DJ, The Cascade Hypothesis of Keratoconus, CLAE, 26(2003);139-146

Figure 1-3 Oxidative Stress (picture courtesy of L. Sorbara)

Progression of KC

The “Global consensus on Keratoconus and Ectatic Disease” by Gomes et al defined progression of KC if at least two of the following three parameters change above the normal noise of the measuring instrument: steepening of the anterior corneal surface, steepening of the posterior corneal surface, thinning and/or an increase in the rate of corneal thickness change from the periphery to the thinnest point. Nevertheless, they agreed that there is no quantitative data to define progression. (25)

The rate of progression is influenced by age as younger patients have a higher rate of progression. (34, 35) Shetty et al. created a score for high risk of progression that includes age, eye rubbing, atopic disease, frequent change of glasses and other factors.(see Table 1-1) (36) All of these aspects can help clinicians to treat their patients more appropriately.

Table 1-1 High-risk characteristics for progression of Keratoconus by Shetty et al (36)

Characteristics	Division	Score
Age (in years)	<20	2
	23-30	1
	>30	0
Eye rubbing	Active	2
	Past history	1
	Absent	0
Atopic eye disease	Active	2
	Past history	1
	Absent	0
Frequent change of glasses	Present	2
	Absent	0
Others	Pregnancy	2
	Downs syndrome	1
	Connective tissue disorders	1
	Retinitis pigmentosa	1
	Lebers congenital amaurosis	1

*Scoring for HRC. >8: High risk of progression, 6-8: Moderate risk of progression, <6: Low risk of progression. HRC: High-risk characteristics

Histopathology

The histopathology of KC has not been completely elucidated yet, but many morphological changes have been reported. Sherwin et al. (37) summarized the variations and alterations in each part of the cornea in his histological assessment of KC which is shown in Figure 1-4. KC eventually affects each corneal layer. In the study of Fernandes et al., a change in epithelial thinning was the most common finding in histopathological studies. (38) Kim et al. described atopic changes not only in the superficial but also in the deeper layers of the epithelium. (39) Cells located at the apex were found to be elongated and arranged in a whorl-like fashion. (40)

Scroggs et al. characterized two groups of KC, "typical" corneas including the ones with one or more breaks in Bowman's layer and "atypical" corneas without breaks. (41) Defects and breaks in Bowman's layer are one of the common features of KC. These vary from simple breaks to large gaps where the epithelium connects directly with the stroma. (42)

Another change of the keratoconic cornea is the thinning of the stroma. Although the thickness of the collagen lamellae stays the same, the number of the lamellae are significantly less compared to normal corneas due to increased protease (enzyme) activity. (43) The density of keratocytes in the stroma have also been found to be lower. (44)

In Descemet's membrane ruptures and folds often occur. (37) The cells of the endothelium sometime show intracellular "dark structures", pleomorphism and elongation. (19) Endothelial cell loss may be connected with ruptures in Descemet's membrane or with increased apoptosis. (45, 46)

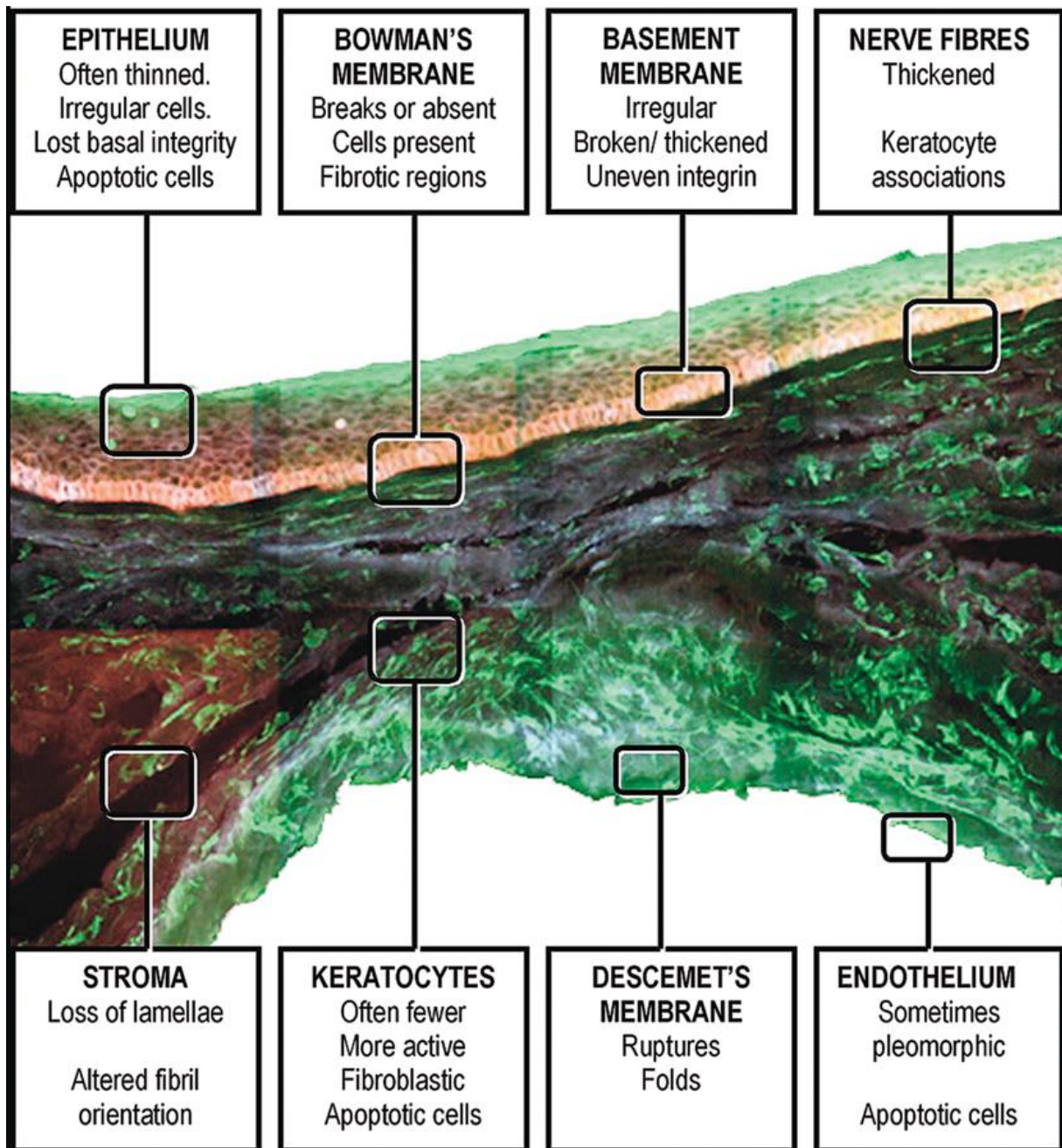


Figure 1-4 Morphological changes in all corneal layers by Sherwin et al (37)

Clinical signs and symptoms

In the early stages of KC, detection may be challenging. There may be no symptoms, only that the patient experiences a deterioration of vision. Due to the thinning, the cornea bulges and induces irregular astigmatism and high myopia. This results in mild to marked impairment of vision. (47)

With the thinning of the cornea, the volume of the cornea decreases. Therefore, some studies propose volume as a factor for detection of KC. (48, 49) Often there can be seen an iron ring around the circumference of the cone (Fleischer's ring) marking the edge of the thinner and thicker cornea and/or fine vertical lines deep in the stroma (Vogt's striae), a buckling of the stroma on itself. (50) KC usually occurs bilaterally but in most cases initially one eye is more greatly affected (leading eye) compared to the other (lagging eye) as the disease progresses asymmetrically. (51) Perry et al. identified two types of cones. (52) The round "nipple" cone is more common, globally and is mostly centrally located whereas the "oval" cone is located more inferiorly or inferior-temporally. (19) In the late stages of KC, corneal scarring may occur over the thinnest point of the cone. (53)

1.2.2 Aberrations with KC

Visual acuity decreases due to corneal aberrations such as spherical aberration, coma and trefoil that the irregularity induces. (47) Keratoconic corneas show higher values of high order aberrations (HOA) compared to normal corneas. Alio et al. suggested considering HOA especially coma-like aberrations in order to grade KC. (54) They assumed that the decentration of the cone in KC significantly increases the coma-like aberrations. There are significant differences among spherical aberration, coma and trefoil comparing normal eyes and eyes with KC. Due to the change in shape and the resulting vertical asymmetry the vertical coma coefficient appears to be one of the best indices to detect early KC. (55)

1.2.3 Management of KC and Corneal Cross linking

In early stages of KC, correction with spectacles or soft contact lenses still might be possible. If KC progresses and the shape of the cornea becomes more irregular, rigid gas permeable lenses (RGP) provide a better optical correction. (56) RGP compensate for the irregular surface of the cornea and therefore increase the quality of vision. Three different fitting philosophies have been practiced in the past but currently the three-point touch method is used the most widely. (57) If for some reason the fitting with RGP is not possible, there are some other options of lens fittings such as soft lenses with increased centre thickness, piggyback, hybrid lenses or scleral lenses. (58, 59) Patients with severe KC who no longer can be corrected with spectacles or contact lenses due to late stage corneal scarring may be referred for a corneal transplant (keratoplasty, either penetrating or lamellar). In many countries, KC is one of the main indications for keratoplasty. (60)

Corneal Cross Linking (CXL) is the only treatment available today for KC to stabilize the cornea and slow its progression. In 2003, Wollensak et al. first evaluated the effect of CXL in human eyes with KC. (61) In the last few years the effect of stopping the progression of KC over various short-term study periods was confirmed by other studies. (62, 63) The cornea is treated with a combination of Riboflavin and Ultraviolet-A-light. Usually UVA light of 370 nm is used because most of this light is absorbed into the cornea and therefore there is no risk to the crystalline lens and the retina. (64)

There are two different ways to proceed with CXL: with either the epithelium-off CXL or trans epithelial CXL (that is epithelium on). In epithelium-off CXL the central epithelium is removed in a 7.00-9.00 mm diameter circle after anaesthetic eye drops are given, (64, 65) whereas, in the trans epithelial CXL, the procedure is performed without removing the epithelium in order to reduce the post-surgical pain that is induced when the epithelium is removed. (66) In both methods, Riboflavin, a photosensitizer, is administered to the cornea. It absorbs the UV irradiation and then generates reactive oxygen species (ROS). These radicals induce the cross linking of the stromal collagen fibrils. (64) The diameter of the collagen fibres in the stroma significantly increase (66) and thereby strengthen the cornea.

Chatzis et al. suggest CXL treatment as soon as possible (63) but most studies focus on patients with only progressive KC as crosslinking of the cornea increases on its own with age due to lifelong UV exposure. (67)

1.2.4 Other corneal disorders

In addition to KC, corneal ectasia can be caused by other aspects. Progressive inferior corneal steepening is one of the complications after laser in situ keratomileusis (LASIK). It is related to an increase in myopia and astigmatism and a loss in vision acuity. (68) Another cause of ectasia with similarities to KC is Pellucid Marginal Degeneration (PMD). PMD is characterized by a narrow band of thinning in the inferior periphery of the cornea with a width of 1-2 mm. It is mostly detected between the second and fifth decade of life and it progresses slowly.(47) PMD is a rare disorder less common than KC but more common than Keratoglobus. (69) Keratoglobus shows a diffuse thinning which is greater in the periphery. This results in a globular shape of the cornea. Unlike PMD or KC, Keratoglobus is non-progressive. (47) As with PMD, Terriens marginal degeneration is a bilateral, slowly progressive thinning in the peripheral cornea. However, the thinning usually starts supero-nasal and is found mostly in patients older than 40 years. (70)

2 Measurement of Corneal Shape

2.1 Topography

Corneal topographic measurements are very common in clinical practice for various purposes. The data may be used for fitting contact lenses as well as for detecting abnormalities in corneal shape as the curvature of the anterior cornea can be directly measured. One of the most common principles of topographic measurement is the specular reflection method. Therefore, a Placido disc system is used. This system consists of several concentric illuminated rings that are reflected onto the cornea (Figure 2-1). From these reflected rings, the corneal curvature is reconstructed and calculated. (71) The first Placido disc was developed in 1880 by Antonio Placido and consisted of alternating black and white concentric bands with a hole in the centre. Antonio Placido took the first photographs of the corneal reflection. (72) In 1984, Klyce presented a computer-based analysis to simplify the interpretation of the images. (73) Computer-assisted videokeratographs (VKE) with high-resolution images were a large step to the digital world at this time. Nowadays instruments such as the Keratograph from Oculus (Wetzlar, Germany) which also consists of a Placido disc with 22 rings and 200 red LEDs automatically use a camera to take multiple images analysed with sophisticated software programs. (74)

Yet, the Placido disc system has some limitations. The curvature can only be measured for 60% of the anterior corneal surface and thus peripheral data is lost. PMD or KC might not be detected as curvature changes can occur posteriorly first. Topographers do not provide data for the posterior surface of the cornea or can they calculate corneal thickness.

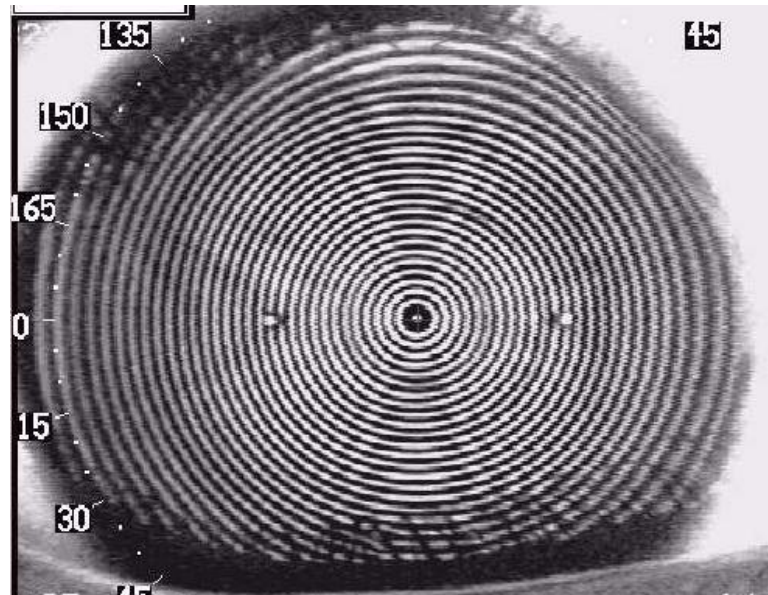


Figure 2-1 Placido disc (picture courtesy of L. Sorbara)

2.2 Tomography

Tomography on the other hand is a projection system that gives a three dimensional image. It is an indirect measure of corneal curvature and shape and is based on elevation maps using a camera system. The imaging process creates a three dimensional image of the anterior eye segment. The elevation maps of both the front and back surface of the cornea are usually shown compared to a reference shape called the best-fit sphere (BFS). (73) From the elevation data of the front and back surface of the cornea, corneal curvature and the pachymetric maps are calculated. (75) There are two different types of tomography methods: slit scanning and Scheimpflug imaging principles.

The Orbscan II from Bausch + Lomb (Rochester, New York, USA) (see Figure 2-2) uses a combination of a Placido disc (corneal curvature) and a slit scanning camera (elevation maps) to describe corneal shape and thickness. 40 slits are projected on the cornea, 20 slits from the right and 20 slits from the left at a fixed angle of 45° to the instrument axis. The camera records the backscattering of the slits from the front and back corneal surfaces and from these data, the structure of the cornea is reconstructed. (76) See Figure 2-3 of a typical pachymetry map of the KC cornea.



Figure 2-2 Orbscan II (picture courtesy of L. Sorbara)

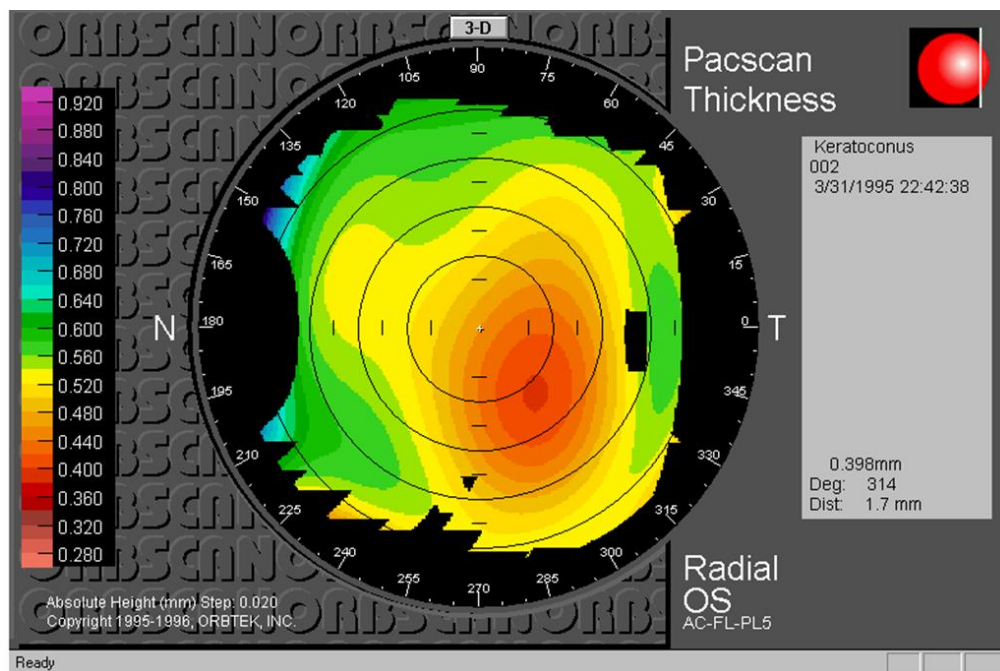


Figure 2-3 Orbscan Pachymetry map (picture courtesy of L. Sorbara)

The Pentacam HR® from Oculus (Wetzlar, Germany) (see Figure 2-4) consists of a camera based on the Scheimpflug principle. The camera is set perpendicular to a slit beam of light. This beam of light rotates 180° around the optical axis of the eye and takes 25 to 50 optic section images of the corneal front and back surface in about 2 seconds. A second camera controls the fixation of the eye and any movement is corrected for. (77) From about 25,000 elevation points, the anterior eye segment is reconstructed. (77) The Pentacam HR® provides not only elevation, curvature and pachymetric data but also data of wave front aberrations and densitometry. (76) See Figure 2-5 as example of a KC cornea showed in the 4 Maps elevation display.



Figure 2-4 Pentacam HR® (picture courtesy of L. Sorbara)

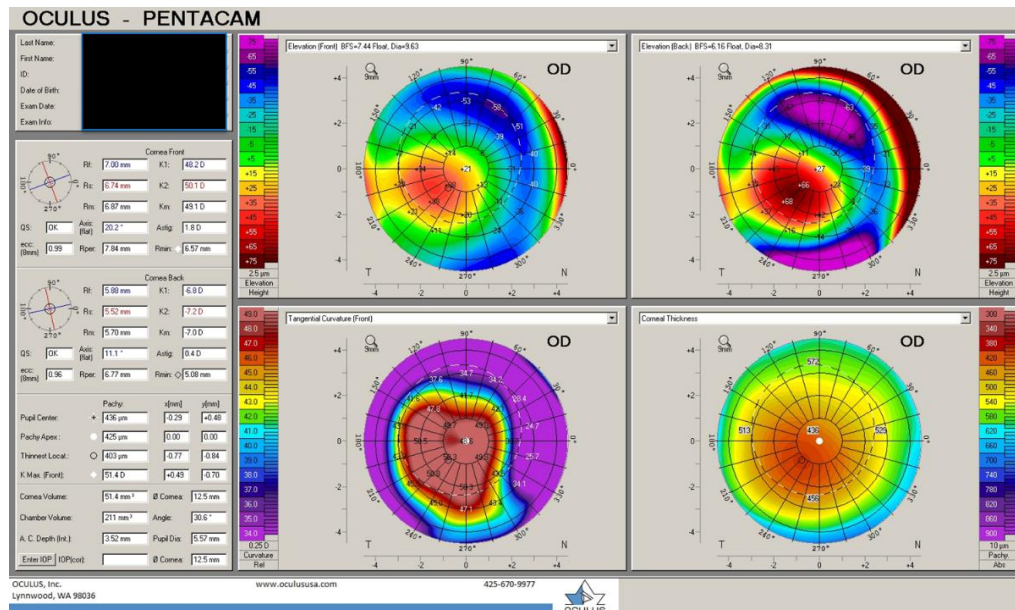


Figure 2-5 Pentacam HR®: 4 Maps display (picture courtesy of L. Sorbara)

The repeatability and reliability of the Pentacam HR has been extensively studied showing that for central thickness after two consecutive readings and on two separate days the instrument was highly repeatable when a single observer. (5, 78) The accuracy of the instrument reduces as the measurements are taken outside of the central region.

2.3 Advantages of Pentacam HR®

The Pentacam HR® is commonly used for KC detection and classification. It measures and calculates data such as the elevation and corneal thickness, which is essential for KC diagnosis.

Firstly, the Pentacam HR® provides the basic information such as the flat and the steep radii of curvature in mm. It measures the elevation data compared to a BFS of both front and back surfaces of the cornea and converts the values into curvature data. For calculating the refractive power (K) in diopters the refractive indices (n) $n=1,3375$ for the anterior surface, $n=1,376$ for the posterior surface of the cornea and $n=1,336$ for the aqueous humor are used. The calculation of the steepest curvature value (Kmax) is based on the sagittal anterior curvature map.

Moreover, the astigmatism of the central cornea and the corneal volume at a diameter of 10 mm around the apex are given. (79)

The Pentacam HR® calculates topographic pachymetry by subtracting the anterior and posterior elevation data at each point of the measured elevations. The thickness and position of the pupil centre, the apex and the thinnest location are given. The positions of the pupil centre and the thinnest location are presented relative to the corneal apex.

The measurements of the Pentacam HR® are based on backscattering light. Normal corneas are transparent and therefore the scatter is small within the cornea. (80) The Pentacam HR® provides a densitometry measurement based on backscatter of the anterior eye segment including the cornea and the lens. The density is given in greyscale units from 0 to 100 which are defined as 0 no backscatter and 100 maximal backscatter. (81) See Figure 2-6 for an example of the density given by the Pentacam HR®.

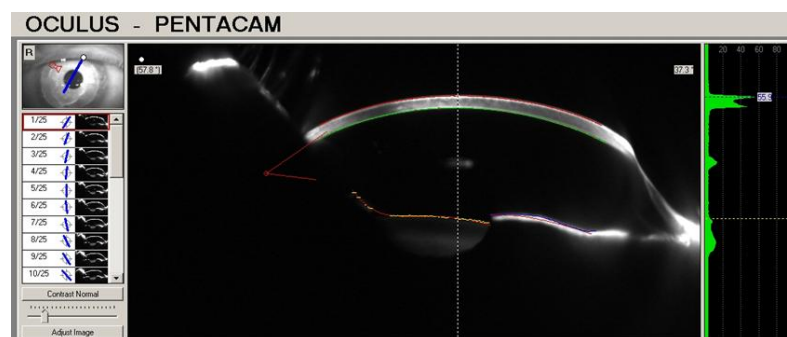


Figure 2-6 Scheimpflug image density (picture courtesy of L. Sorbara)

Important for detecting KC are the eight topometric indices that the Pentacam HR® provides. These indices are calculated with data from curvature data, elevation and data from Zernike analysis in an 8 mm zone of the central cornea. (79)

Curvature Based Indices

The Index of Surface Variance (ISV) is unit less and measures the deviation of the individual corneal radii from the median value. It increases if there are irregularities. The Index of Vertical Asymmetry (IVA) measures the symmetry of the superior and inferior curvature with the horizontal meridian as a mirroring axis in mm. (82) It increases with astigmatism, KC or limbal ectasia. The Keratoconus Index (KI) shows the ratio between superior and inferior mean radius values and is increased especially for KC. The Central Keratoconus Index (CKI) expresses the ratio between central and peripheral mean radius values and increases especially for central KC. RMin is the smallest sagittal radius given in mm. It is decreased for KC. (79, 82)

Elevation Based Indices

The Index of Height Asymmetry (IHA) measures the symmetry of elevation with horizontal meridian as axis of reflection in μm . It is similar to the IVA but in some cases more sensitive. The Index of Height Decentration (IHD) calculates the decentration of elevation in vertical direction from a Fourier Analysis on a ring of 3 mm radius. It is expressed in μm and is increased for KC. (79, 82)

The Topographical Keratoconus Classification (TKC) gives the grade of the KC based on the Amsler-Krumeich Classification (83) with using just the anterior surface shown in Table 2-1.

Table 2-1 Amsler-Krumeich classification (adapted from Krumeich et al (83))

Stage I	Eccentric steepening Myopia, induced astigmatism, or both <5.00 D Mean central K readings <48 D
Stage II	Myopia, induced astigmatism, or both from 5.00 to 8.00 D Mean central K readings <53.00 D Absence of scarring Corneal thickness >400 micron
Stage III	Myopia, induced astigmatism, or both from 8.00 to 10.00 D Mean central K readings >53.00 D Absence of scarring Corneal thickness 300 – 400 micron
Stage IV	Refraction not measurable Mean central K readings >55.00 D Central corneal scarring Corneal thickness < 300 micron

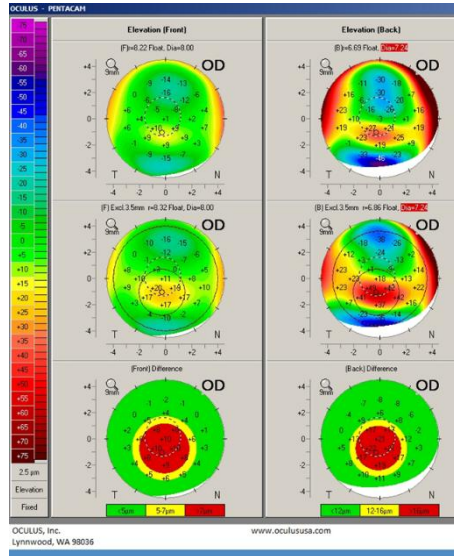
The Indices (except TKC) are shown in white if the deviation is smaller than 2.5 standard deviation (SD), yellow if it ranges between 2.5 and 3 SD and red if it is larger than 3 SD. The limiting values are shown in Table 2-2. The SD is based on a database used for comparison to the normal population. (79)

Table 2-2 Limiting values for topographic indices (adapted from the Pentacam User Manual (79))

Index	Abnormal (Yellow)	Pathological (Red)
ISV (Index of Surface Variance)	≥ 37	≥ 41
IVA (Index of Vertical Asymmetry)	≥ 0.28	≥ 0.32
KI (Keratoconus Index)	> 1.07	> 1.07
CKI (Central Keratoconus Index)	≥ 1.03	≥ 1.03
Rmin	< 6.71	< 6.71
IHA (Index of Height Asymmetry)	≥ 19	> 21
IHD (Index of Height Decentration)	≥ 0.014	≥ 0.016

Elevation and Pachymetry Based Indices

The Belin-Ambrosio Enhanced Ectasia Display (BAD) is a comprehensive display of the Pentacam HR® that combines elevation and pachymetry data Figure 2-7. It shows the elevation data for the front and the back surface of the cornea in reference to a BFS calculated at a central 8 mm zone. In eyes with ectasia the cone steepens the BFS and reduces the actual elevation difference. The "enhanced reference surface" presents the elevation data in reference to a BFS that is calculated at the 8 mm zone excluding the data of a 3.5 mm zone around the thinnest point. In normal eyes the excluding of the thinnest point shows little difference but in eyes with ectasia the protrusion can be seen more precisely. In the third map the display shows the change between the baseline elevation and the enhanced elevation map. (84)



Furthermore, the pachymetry of the thinnest point and the apex are given and the displacement of the thinnest point to the apex is calculated. Eyes with KC show a higher displacement compared to the reference population. The progression of the thickness is measured from the thinnest location to the periphery in 22 concentric rings. One graph shows the "Corneal Thickness Spatial Profile" and a second one the "Percentage Thickness Increase" (Figure 2-8). Both graphs provides a line of the average progression in normal population and ± 2 SD. Ectatic eyes thin faster from the periphery to the thinnest point. (84)

The BAD performs a regression analysis against a standard database for each value (change in anterior elevation, change in posterior elevation, corneal thickness at the thinnest point, thinnest point displacement and pachymetric progression). It also provides five new parameters for the front surface (Df), the back surface (Db), the pachymetry progression (Dp), the thinnest point (Dt) and the thinnest point displacement (Da or Dy(83)). The D-index is a final overall index including all five parameters. If the values are < 1.6 SD the parameters are shown in white, ≥ 1.6 in yellow, ≥ 2.6 in red. (84)

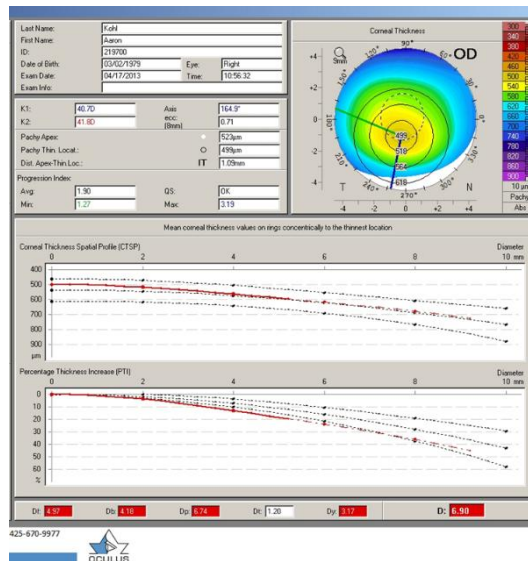


Figure 2-8 BAD display pachymetry data (picture courtesy of L. Sorbara)

The ABCD grading is a new classification system introduced by M. W. Belin and J.K. Duncan. (85) It has similarities to the Amsler-Krumeich classification (83) but is based on tomography and includes also the posterior surface of the cornea and the visual acuity. The four parameters are the anterior radius of curvature (A), posterior radius of curvature (B), corneal pachymetry at thinnest (C) and Distance best corrected vision (D). The radii are calculated for a 3 mm zone with the thinnest point as the centre. Furthermore, the ABCD gradings add stage 0 as a fifth stage to distinguish eyes without KC. (85)

Table 2-3 ABCD grading system adapted by Belin et al. (85) (anterior and posterior radius of curvature (ARC, PRC), best corrected distance visual acuity (BDVA))

ABCD criteria	A ARC (3mm Zone)	B PRC (3mm Zone)	C Thinnest μm pach	D BDVA
Stage 0	7.25mm (> 46.5 D)	> 5.90mm	> 490 μm	≥ 20/20 (≥1.0)
Stage I	7.05mm (< 48.0 D)	> 5.70mm	> 450 μm	< 20/20 (< 1.0)
Stage II	> 6.35mm (< 53.0 D)	> 5.15mm	> 400 μm	< 20/40 (< 0.5)
Stage III	> 6.15mm (< 55.0 D)	> 4.95mm	> 300 μm	< 20/100 (< 0.2)
Stage IV	< 6.15mm (> 55.0 D)	< 4.95mm	≤ 300 μm	< 20/400 (< 0.05)

Another advantage compared to other tomographers is the measurement of the wave front aberrations. Using the elevation data the Pentacam HR® performs the Zernike Analysis for the front and back surface of the cornea. It provides Zernike coefficients for the anterior, the posterior and the complete cornea up to Zernike polynomial degree 8. (79)

All of these indices were created by comparing to normal population with the aim to detect and diagnose KC in early stages.

3 The Study

3.1 Purpose and Motivation

The purpose of this study is to see which indices of the Pentacam HR® are sensitive enough to detect change in the keratoconic cornea. Knowing the progression of KC over shorter periods will direct the management of the patients regarding surgical procedures such as CXL.

For that reason it would be informative to know which of the indices that the Pentacam HR® calculates are predictive and correlate with the progression of KC compared to the normal population. The control group data was from a sample of convenience as they were optometry students at the University of Waterloo, School of Optometry and Vision Science.

3.2 Objectives

The main purpose of the study is answer the following questions:

1. Do the indices that the Pentacam HR® give change enough to detect progression of KC when examining longitudinal data?
2. Which indices are the best predictors of the changes over time?
3. Do these indices correlate with age, the stage of KC, presence of atopic (systemic) disease and whether or not corneal cross-linking was performed?

3.3 Hypothesis

The hypothesis is that some indices will not be as predictive to KC progression as others will. Indices will include K max, corneal curvature, corneal thickness, corneal volume and density, corneal aberrations and elevation data and how these correlate with predictor variables such as age, stage of KC, corneal cross-linking and associated systemic and ocular conditions.

3.4 Study design

Retrospective chart review from the Pentacam HR® instrument and the electronic medical record (demographic data) were used.

3.5 Participants

Participants who had signed the SOVS clinic consenting to a chart review were included that fell into our 2 study groups. The participants were divided into the test group including eyes diagnosed with KC and the control group including normal eyes.

3.5.1 Sample size calculation

As this study will be exploratory in nature, no previous data are available. Therefore, no sample size calculation is possible. Due to the lower prevalence of KC at least 100 cases would need to be examined to show progression.

3.5.2 Number of participants

106 keratoconic participants and 28 controls were recruited using contact lens clinic records at the University of Waterloo. Eligibility were determined using the inclusion and exclusion criteria detailed below for the KC group. Participants have signed/agreed to the Teaching and Research Permission Form used by the SOVS Clinic prior to their information being accessed (Appendix 1). Data from a maximum of three imaging sessions over a three year period was collected. This study was performed under the Tenets of Helsinki and under the University of Waterloo, Research Ethics Board.

3.5.3 Inclusion and exclusion criteria

A person is eligible for inclusion in the study if he/she:

1. Has read and signed the Teaching and Research Permission Form.
2. Has been diagnosed with keratoconus for the test group and has not been diagnosed with KC for the control groups.

A person will be excluded from the study if he/she:

1. Has had any other corneal surgery except CXL.

3.6 Statistical Analysis

All data was analyzed by STATISTICA 7 (StatSoft, Tulsa, OK). The indices were tested for normality. To compare between the groups, if the indices were normally distributed the unpaired t-test was used and if they were not the Mann-Whitney U test was used. For the comparison between the visits within each group the paired t-test or the Wilcoxon test was used. All tests were performed with $\alpha \leq 0.05$.

3.7 Results Part I

3.7.1 Demographic

Data of 182 eyes of 106 participants with KC were collected from the Pentacam HR®. 139 participants were male (76.37%) and 43 were female (23.63%). The average age was 39.15 (± 12.78) years. 90 eyes were right eyes (49.45%) and 92 were left eyes (50.55%).

The eyes were divided into one group including eyes that have undergone CXL and into a second group with eyes without CXL. After age matching these two groups there were a total of 36 eyes in each group. The age was not significantly different ($p=0.355$). The demographics are shown in Table 3-1. There was insufficient data for the third visit and therefore all participants who had two visits were included in the data analysis. The mean time difference in years between the first visit (V1) and the second visit (V2) is given in Table 3-2 where there was a significant difference in the time over which the data was collected ($p=0.037$) as the CXL patients were monitored more frequently.

Table 3-1 Demographics of CXL and Non CXL

n=36	CXL	Non CXL
Mean Age (years)	30.25	32.53
SD Age (years)	10.88	9.55
Male (%)	80.56	77.78
Female (%)	19.44	22.22
OD (%)	55.56	47.22
OS (%)	44.44	52.78

Table 3-2 Mean time difference between visits for CXL and Non CXL

n=36	CXL	Non CXL	p value (t-test)
Mean V1-V2	1.37	1.83	0.037
SD V1-V2	0.87	0.94	

For comparison 28 normal eyes of participants without KC were analysed. Data of a first and second visit was collected. The mean time difference between the two visits was 1.17 (± 0.70) years. They were age matched to 28 KC participants with CXL and 28 KC participants without CXL. Their demographics are shown in Table 3-3. The age between the control group and the CXL group was not significantly different ($p=0.611$). The age of the Non CXL group was significantly different compared to the control ($p<0.001$) and to the CXL group ($p<0.001$). The mean time between the first and the second visit in the Non CXL group was 1.96 (± 0.96) years and in the CXL group 1.29 (± 0.63) years as shown in Table 3-4 where again the CXL and normal groups were seen more frequently and within the same time frame.

Table 3-3 Demographics Control, Non CXL and CXL

n=28	Normal	Non CXL	CXL
Mean Age (years)	25.56	27.79	23.00
SD Age (years)	8.06	2.98	2.46
Male (%)	28.57	71.43	85.71
Female (%)	71.43	28.57	14.29
OD (%)	67.86	46.43	53.57
OS (%)	32.14	53.57	46.43

Table 3-4 Mean time difference between V1 and V2 T-Test

n=28	p
Normal vs. Non CXL	0.004
Normal vs. CXL	0.486
Non CXL vs. CXL	0.001

3.7.2 Leading and lagging eye

All 182 keratoconic eyes were divided into 2 groups of 91 eyes. Group 1 includes the lagging eyes with $K_{max} \leq 51.1$ D and Group 2 includes the leading eyes with $K_{max} \geq 51.1$ D. In Group 1 43.96% and in Group 2 54.95% are right eyes. As it is shown in Table 3-5 they are significantly different ($p<0.05$, all). Therefore, in the following study right and left eyes of the KC patients are used.

Table 3-5 Comparing leading eye and lagging eye

	Mean	Std.Dv.	Diff.	Std.Dv. Diff.	t	df	p
K max (D) G1	48.65	2.94					
K max (D) G2	59.80	6.49	-11.15	4.32	-24.64	90	<0,0001
K flat (D) G1	43.38	2.66					
K flat (D) G2	49.16	5.83	-5.78	4.95	-11.14	90	<0,0001
K steep (D) G1	45.78	2.51					
K steep (D) G2	53.14	5.88	-7.36	4.59	-15.28	90	<0,0001
Ast (D) G1	2.26	1.48					
Ast (D) G2	3.97	1.95	-1.71	2.29	-7.12	90	<0,0001
Pupil centre (µm) G1	511.18	49.64					
Pupil centre (µm) G2	473.97	52.40	37.21	69.05	5.14	90	<0,0001

3.7.3 Influence of systemic disease

The keratoconic eyes were divided into two groups. Group 1 including 51 eyes of participants with atopic disease and Group 2 including 51 eyes of participants without any systemic disease. All eyes that had undergone CXL had been excluded and the groups were age matched. The age was not significantly different ($p=0.363$). The demographics are shown in Table 3-6.

Table 3-6 Demographics of participants with and without atopic disease

	Group 1	Group 2
Mean Age (years)	45.35	43.51
SD Age (years)	9.95	10.76
Male (%)	64.71	74.51
Female (%)	35.29	25.49
OD (%)	50.98	54.9
OS (%)	40.02	45.1

There was no significant difference between the two groups ($p>0.05$, all) (see Table 3-7 and Table 3-8)

Table 3-7 With (Group 1) and Without (Group 2) atopic disease Visit 1

n=51 df=99	T-test						Mann-Whitney U test		
Visit 1	Mean Group 1	Mean Group 2	t-value	p	SD Group 1	SD Group 2		p	Mann-Whitney U
Curvature									
K max (D)	53.84	53.96	-0.08	0.933	7.26	7.05	ISV	0.726	1223.5
K flat (D)	46.37	46.49	-0.11	0.911	5.32	5.41	IVA (mm)	0.841	1245.5
K steep (D)	49.36	49.72	-0.32	0.752	5.59	5.92	KI	0.627	1203.5
Ast (D)	2.97	3.23	-0.69	0.492	1.89	1.89	CKI	0.583	1194.5
Rmin (mm)	6.37	6.35	0.11	0.914	0.76	0.76			
Elevation									
BFS Front (mm)	7.33	7.34	-0.14	0.886	0.48	0.51	A (0 to 4)	0.846	1246.5
BFS Back (mm)	6.01	5.98	0.33	0.740	0.47	0.52	B (0 to 4)	0.526	1189
Df	8.64	9.21	-0.35	0.729	6.93	9.40	IHA (µm)	0.245	1104
Db	7.89	8.29	-0.29	0.769	6.63	7.09	IHD (µm)	0.582	1194
Pachymetry									
Pupil centre pachymetry (µm)	501.80	487.64	1.38	0.172	53.76	49.57	C (0 to 4)	0.573	1192
x Pupil centre (mm)	0.02	0.04	-0.38	0.707	0.20	0.23			
y Pupil centre (mm)	0.34	0.31	0.54	0.591	0.37	0.23			
Apex Pachymetry (µm)	489.18	477.00	1.05	0.296	60.27	56.11			
Thinnest location pachymetry (µm)	463.55	453.92	0.76	0.450	68.60	58.46			
x Thinnest location (mm)	0.03	-0.02	0.37	0.713	0.69	0.69			
y Thinnest location (mm)	-0.89	-0.83	-0.51	0.613	0.58	0.47			
Corneal volume (qmm)	58.81	58.41	0.50	0.616	4.29	3.63			
Dp	12.81	12.25	0.23	0.820	13.76	10.85			
Dt	2.90	3.18	-0.50	0.619	3.02	2.71			
Da	2.89	3.13	-1.35	0.180	1.09	0.67			
Aberrations									
Coma 90° (µm)	-1.60	-1.38	-0.92	0.358	1.13	1.33			
Coma 0° (µm)	0.01	0.03	-0.10	0.924	0.98	1.13			
Trefoil (µm)	-0.07	0.06	-1.67	0.099	0.49	0.29			
Spherical aberration (µm)	-0.10	-0.14	0.30	0.763	0.74	0.70			
Density									
Density 90°	38.56	39.60	-0.38	0.704	11.01	15.97			
Density 180°	40.36	38.44	0.65	0.516	14.74	14.94			
D	9.45	9.37	0.07	0.944	6.47	5.65	TKC (0-4)	0.654	1210

Table 3-8 With (Group 1) and without (Group 2) atopic disease Visit 2

n=51 df=99	T-test						Mann-Whitney U test		
Visit 2	Mean Group 1	Mean Group 2	t-value	p	SD Group 1	SD Group 2		p	Mann-Whitney U
Curvature									
K max (D)	54.35	53.85	0.31	0.760	8.83	7.43	ISV	0.654	1209
K flat (D)	46.79	46.93	-0.11	0.910	6.43	5.63	IVA (mm)	0.905	1257.5
K steep (D)	49.73	49.88	-0.12	0.904	6.60	6.17	KI	0.734	1225
Ast (D)	2.93	2.91	0.05	0.959	1.87	1.93	CKI	0.495	1175
Rmin (mm)	6.35	6.38	-0.17	0.862	0.89	0.76			
Elevation									
BFS Front (mm)	7.32	7.34	-0.15	0.880	0.52	0.50	A (0 to 4)	0.720	1222.5
BFS Back (mm)	6.02	6.02	-0.02	0.986	0.48	0.46	B (0 to 4)	0.492	1180.5
Df	9.71	9.38	0.17	0.864	9.59	9.67	IHA (µm)	0.347	1136.5
Db	8.32	8.39	-0.04	0.966	7.95	7.70	IHD (µm)	0.773	1232.5
Pachymetry									
Pupil centre pachymetry (µm)	505.14	490.68	1.46	0.148	50.11	49.56	C (0 to 4)	0.627	1203.5
x Pupil centre (mm)	0.04	0.04	-0.02	0.988	0.24	0.25			
y Pupil centre (mm)	0.40	0.31	1.38	0.170	0.38	0.25			
Apex Pachymetry (µm)	487.27	480.12	0.60	0.548	61.10	58.23			
Thinnest location pachymetry (µm)	461.98	458.08	0.31	0.760	69.63	57.86			
x Thinnest location (mm)	0.04	-0.12	1.19	0.237	0.68	0.70			
y Thinnest location (mm)	-0.86	-0.73	-1.17	0.246	0.59	0.58			
Corneal volume (qmm)	58.27	58.66	-0.50	0.616	3.89	3.96			
Dp	12.64	11.97	0.24	0.809	15.87	11.37			
Dt	2.94	3.01	-0.10	0.919	3.39	2.63			
Da	2.93	3.08	-0.88	0.383	0.97	0.66			
Aberrations									
Coma 90° (µm)	-1.71	-1.36	-1.40	0.165	1.29	1.23			
Coma 0° (µm)	0.02	0.03	-0.04	0.965	1.04	1.18			
Trefoil (µm)	-0.12	0.05	-1.63	0.107	0.63	0.40			
Spherical aberration (µm)	-0.16	-0.19	0.20	0.843	0.84	0.73			
Density									
Density 90°	36.14	38.87	-1.25	0.212	10.42	11.40			
Density 180°	36.79	38.79	-0.79	0.429	12.02	13.21			
D	9.63	9.31	0.24	0.810	7.50	5.82	TKC (0-4)	0.563	1191

Comparing the atopic group from visit 1 to visit 2, IHD (p=0.0038) increased and the Kmax steepened although not significantly. Comparing the first and second visit of the group without atopic disease the Kmax flattened but not significantly, although a significant change was found in the flat K (p=0.0005) as it steepened, pachymetry (p=0.0068) where thickening occurred, back surface BFS as it became flatter (p=0.0375) and IHD which increased (p=0.0007).

3.7.4 Comparing Normal to Non CXL to CXL

The Control group and the Non CXL group were significantly different at each visit for all the measured factors ($p < 0.05$, all) except in the horizontal location of the pupil centre, the position of the thinnest location, Coma 0° and Trefoil ($p > 0.05$, all) (see Table 3-9 and Table 3-10). Of note, there was a significant difference found in densitometry where the ranges of the values in the 090th meridian were found to be: normals (24.9 to 33.3, with an outlier removed) and 25.4 to 55.2, with outlier removed in the Non CXL group at Visit 1.

Table 3-9 Normal compared to Non CXL Visit 1

n=28 df=54	T-test						Mann-Whitney U test		
Visit 1	Mean Normal	Mean Non CXL	t-value	p	SD Normal	SD Non CXL		p	Mann-Whitney U
Curvature									
K max (D)	44.56	51.93	-7.12	<0.001	1.15	5.35	ISV	<0.001	11.5
K flat (D)	42.91	44.56	-2.91	0.005	1.09	2.79	IVA (mm)	<0.001	1.5
K steep (D)	44.15	47.79	-5.37	<0.001	1.09	3.42	KI	<0.001	30
Ast (D)	1.23	3.22	-4.67	<0.001	0.68	2.15	CKI	<0.001	171.5
Rmin (mm)	7.58	6.57	7.69	<0.001	0.19	0.67			
Elevation									
BFS Front (mm)	7.83	7.61	3.50	0.001	0.18	0.28	A (0 to 4)	<0.001	98.5
BFS Back (mm)	6.36	6.20	2.93	0.005	0.16	0.24	B (0 to 4)	<0.001	34
Df	-0.14	7.80	-7.46	<0.001	0.86	5.56	IHA (µm)	<0.001	139.5
Db	-0.15	6.19	-7.63	<0.001	0.58	4.28	IHD (µm)	<0.001	3
Pachymetry									
Pupil centre pachymetry (µm)	548.29	491.79	5.11	<0.001	33.90	47.74	C (0 to 4)	<0.001	76
x Pupil centre (mm)	0.02	0.05	-0.49	0.627	0.17	0.22			
y Pupil centre (mm)	0.07	0.27	-4.42	<0.001	0.12	0.21			
Apex Pachymetry (µm)	548.04	485.68	5.48	<0.001	33.05	50.28			
Thinnest location pachymetry (µm)	543.54	467.32	6.38	<0.001	34.09	53.25			
x Thinnest location (mm)	-0.26	0.04	-1.80	0.077	0.50	0.72			
y Thinnest location (mm)	-0.46	-0.63	2.30	0.025	0.19	0.33			
Corneal volume (qmm)	61.99	57.67	4.10	<0.001	3.70	4.17			
Dp	1.00	8.45	-6.66	<0.001	0.72	5.87			
Dt	-0.11	2.55	-6.35	<0.001	0.93	2.00			
Da	0.63	2.79	-10.57	<0.001	0.56	0.92			
Aberrations									
Coma 90° (µm)	0.01	-1.47	7.24	<0.001	0.15	1.08			
Coma 0° (µm)	0.02	0.02	0.01	0.992	0.10	0.69			
Trefoil (µm)	0.00	0.08	-1.29	0.202	0.08	0.31			
Spherical aberration (µm)	0.20	-0.19	4.00	<0.001	0.08	0.51			
Density									
Density 90°	30.64	35.22	-1.93	0.058	8.40	9.31			
Density 180°	30.19	35.95	-2.34	0.023	8.67	9.69			
D	1.00	7.50	-8.89	<0.001	0.46	3.84	TKC (0-4)	<0.001	56

There was also a significant difference found in densitometry where the ranges of the values in the 090th meridian were found to be: normals (24.8 to 33.7) and 27.2 to 53.6, with outlier removed in the Non CXL group at Visit 2.

Table 3-10 Normal compared to Non CXL Visit 2

n=28 df=54	T-test						Mann-Whitney U test		
Visit 2	Mean Normal	Mean Non CXL	t-value	p	SD Normal	SD Non CXL		p	Mann-Whitney U
Curvature									
K max (D)	44.54	52.15	-7.18	<0.001	1.18	5.49	ISV	<0.001	10.5
K flat (D)	42.71	44.94	-3.73	<0.001	1.24	2.91	IVA (mm)	<0.001	5
K steep (D)	44.03	47.85	-5.56	<0.001	1.26	3.41	KI	<0.001	19
Ast (D)	1.26	2.92	-4.31	<0.001	0.75	1.90	CKI	<0.001	133
Rmin (mm)	7.58	6.54	7.91	<0.001	0.20	0.67			
Elevation									
BFS Front (mm)	7.86	7.58	3.93	<0.001	0.22	0.30	A (0 to 4)	<0.001	82
BFS Back (mm)	6.39	6.22	3.08	0.003	0.17	0.23	B (0 to 4)	<0.001	23
Df	-0.33	7.87	-7.93	<0.001	0.89	5.40	IHA (µm)	<0.001	77
Db	-0.29	6.19	-8.20	<0.001	0.64	4.13	IHD (µm)	<0.001	2.5
Pachymetry									
Pupil centre pachymetry (µm)	548.61	495.04	5.22	<0.001	31.45	44.27	C (0 to 4)	<0.001	83
x Pupil centre (mm)	0.01	0.05	-0.82	0.418	0.18	0.18			
y Pupil centre (mm)	0.07	0.28	-4.32	<0.001	0.11	0.24			
Apex Pachymetry (µm)	548.39	489.00	5.70	<0.001	30.57	45.84			
Thinnest location pachymetry (µm)	542.25	472.86	6.34	<0.001	32.57	47.93			
x Thinnest location (mm)	-0.31	0.05	-2.03	0.048	0.60	0.71			
y Thinnest location (mm)	-0.50	-0.62	1.64	0.107	0.21	0.31			
Corneal volume (qmm)	61.90	57.77	4.22	<0.001	3.41	3.90			
Dp	1.16	7.15	-7.51	<0.001	0.76	4.15			
Dt	-0.07	2.29	-6.41	<0.001	0.91	1.72			
Da	0.77	2.74	-10.04	<0.001	0.65	0.82			
Aberrations									
Coma 90° (µm)	0.01	-1.55	7.43	<0.001	0.20	1.09			
Coma 0° (µm)	0.01	-0.04	0.37	0.712	0.10	0.72			
Trefoil (µm)	-0.01	0.00	-0.15	0.884	0.17	0.30			
Spherical aberration (µm)	0.20	-0.23	4.18	<0.001	0.12	0.53			
Density									
Density 90°	28.73	37.52	-4.10	<0.001	2.01	11.18			
Density 180°	28.20	36.95	-3.69	<0.001	2.16	12.37			
D	1.07	7.21	-9.20	<0.001	0.46	3.50	TKC (0-4)	<0.001	42

Comparing the first visit of the Control group and the CXL group all parameters and indices are significantly different ($p < 0.05$, all). (see Table 3-11) In the second visit the horizontal location of the pupil centre, the location of the thinnest location, Coma 0° and Trefoil were not different ($p > 0.05$) but the rest of the factors were significantly different ($p < 0.05$, all). (see Table 3-12) There was a significant difference found in densitometry where the ranges of the values in the 090th meridian were found to be: normals (24.9 to 33.3, with an outlier removed) and 25.7 to 65.4, with outlier removed in the CXL group at Visit 1.

Table 3-11 Normal compared to CXL Visit 1

n=28 df=54	T-test						Mann-Whitney U test		
Visit 1	Mean Normal	Mean CXL	t-value	p	SD Normal	SD CXL		p	Mann-Whitney U
Curvature									
K max (D)	44.56	56.16	-7.31	<0.001	1.15	8.31	ISV	<0.001	8
K flat (D)	42.91	46.79	-3.48	<0.001	1.09	5.78	IVA (mm)	<0.001	2
K steep (D)	44.15	49.78	-4.39	<0.001	1.09	6.70	KI	<0.001	3
Ast (D)	1.23	2.94	-4.09	<0.001	0.68	2.10	CKI	<0.001	99.5
Rmin (mm)	7.58	6.12	9.11	<0.001	0.19	0.82			
Elevation									
BFS Front (mm)	7.83	7.39	3.63	<0.001	0.18	0.62	A (0 to 4)	<0.001	55.5
BFS Back (mm)	6.36	5.99	3.08	<0.001	0.16	0.62	B (0 to 4)	<0.001	57
Df	-0.14	11.29	-8.02	<0.001	0.86	7.50	IHA (µm)	<0.001	114
Db	-0.15	10.07	-6.87	<0.001	0.58	7.71	IHD (µm)	<0.001	0
Pachymetry									
Pupil centre pachymetry (µm)	548.29	495.14	4.28	<0.001	33.90	56.29	C (0 to 4)	<0.001	82
x Pupil centre (mm)	0.02	0.03	-0.21	<0.001	0.17	0.16			
y Pupil centre (mm)	0.07	0.25	-3.14	<0.001	0.12	0.29			
Apex Pachymetry (µm)	548.04	485.21	5.14	<0.001	33.05	55.54			
Thinnest location pachymetry (µm)	543.54	465.64	5.94	<0.001	34.09	60.42			
x Thinnest location (mm)	-0.26	-0.12	-0.99	<0.001	0.50	0.59			
y Thinnest location (mm)	-0.46	-0.70	3.38	<0.001	0.19	0.33			
Corneal volume (qmm)	61.99	59.66	1.86	<0.001	3.70	5.50			
Dp	1.00	12.10	-5.40	<0.001	0.72	10.86			
Dt	-0.11	2.70	-5.55	<0.001	0.93	2.51			
Da	0.63	3.04	-12.35	<0.001	0.56	0.87			
Aberrations									
Coma 90° (µm)	0.01	-1.94	8.52	<0.001	0.15	1.20			
Coma 0° (µm)	0.02	-0.13	1.21	<0.001	0.10	0.67			
Trefoil (µm)	0.00	0.08	-1.19	<0.001	0.08	0.36			
Spherical aberration (µm)	0.20	-0.36	4.52	<0.001	0.08	0.65			
Density									
Density 90°	30.64	40.09	-3.51	<0.001	8.40	11.49			
Density 180°	30.19	41.23	-3.62	<0.001	8.67	13.61			
D	1.00	10.01	-9.00	<0.001	0.46	5.27	TKC (0-4)	<0.001	42

There was a significant difference found in densitometry where the ranges of the values in the 090th meridian were found to be: normals (24.8 to 33.7) and 26.8 to 84.6, with outlier removed in the CXL group at Visit 2. (see Table 3-12)

Table 3-12 Normal compared to CXL Visit 2

n=28 df=54	T-test						Mann-Whitney U test		
Visit 2	Mean Normal	Mean CXL	t-value	p	SD Normal	SD CXL		p	Mann-Whitney U
Curvature									
K max (D)	44.54	56.74	-8.26	<0.001	1.18	7.73	ISV	<0.001	11
K flat (D)	42.71	47.22	-4.08	<0.001	1.24	5.71	IVA (mm)	<0.001	2.5
K steep (D)	44.03	50.90	-5.22	<0.001	1.26	6.86	KI	<0.001	1.5
Ast (D)	1.26	3.20	-4.27	<0.001	0.75	2.29	CKI	<0.001	20.5
Rmin (mm)	7.58	6.05	9.99	<0.001	0.20	0.79			
Elevation									
BFS Front (mm)	7.86	7.34	3.95	<0.001	0.22	0.65	A (0 to 4)	<0.001	42.5
BFS Back (mm)	6.39	5.97	3.42	0.001	0.17	0.62	B (0 to 4)	<0.001	31.5
Df	-0.33	11.61	-10.14	<0.001	0.89	6.17	IHA (µm)	<0.001	156
Db	-0.29	10.05	-8.45	<0.001	0.64	6.44	IHD (µm)	<0.001	0
Pachymetry									
Pupil centre pachymetry (µm)	548.61	488.71	4.90	<0.001	31.45	56.58	C (0 to 4)	<0.001	67.5
x Pupil centre (mm)	0.01	0.04	-0.80	0.430	0.18	0.15			
y Pupil centre (mm)	0.07	0.35	-5.64	<0.001	0.11	0.24			
Apex Pachymetry (µm)	548.39	476.29	5.71	<0.001	30.57	59.37			
Thinnest location pachymetry (µm)	542.25	458.71	6.29	<0.001	32.57	62.25			
x Thinnest location (mm)	-0.31	-0.03	-1.74	0.088	0.60	0.62			
y Thinnest location (mm)	-0.50	-0.67	1.39	0.170	0.21	0.60			
Corneal volume (qmm)	61.90	58.98	2.44	0.018	3.41	5.34			
Dp	1.16	12.14	-5.29	<0.001	0.76	10.95			
Dt	-0.07	3.03	-5.36	<0.001	0.91	2.93			
Da	0.77	3.10	-12.26	<0.001	0.65	0.77			
Aberrations									
Coma 90° (µm)	0.01	-1.97	7.15	<0.001	0.20	1.45			
Coma 0° (µm)	0.01	-0.05	0.39	0.696	0.10	0.79			
Trefoil (µm)	-0.01	0.00	-0.20	0.841	0.17	0.35			
Spherical aberration (µm)	0.20	-0.51	5.24	<0.001	0.12	0.70			
Density									
Density 90°	28.73	45.75	-4.47	<0.001	2.01	20.05			
Density 180°	28.20	44.26	-4.23	<0.001	2.16	19.99			
D	1.07	10.07	-9.67	<0.001	0.46	4.91	TKC (0-4)	<0.001	28

For the normal group, between the first and the second visit some of the parameters and indices changed significantly: curvature based indices-ISV and IVA, elevation based BFS (back) (p=0.046), IHA and IHD, pachymetry based indices-the y-coordinate of the thinnest location, Dp and Da (p<0.05, all). (see Table 3-13)

Table 3-13 Normal V1 compared to V2

n=28	T-test			Wilcoxon Test	
	Mean difference	t-value	p		p
Curvature					
K max (D)	0.03	0.42	0.675	ISV	0.009
K flat (D)	0.20	2.05	0.050	IVA (mm)	0.014
K steep (D)	0.12	1.28	0.213	KI	0.639
Ast (D)	-0.03	-0.42	0.677	CKI	0.641
Rmin (mm)	-0.01	-0.53	0.599		
Elevation					
BFS Front (mm)	-0.03	-1.61	0.118	A (0 to 4)	
BFS Back (mm)	-0.02	-2.10	0.046	B (0 to 4)	
Df	0.19	1.70	0.101	IHA (μm)	0.019
Db	0.16	1.88	0.071	IHD (μm)	0.008
Pachymetry					
Pupil centre pachymetry (μm)	-0.32	-0.16	0.872	C (0 to 4)	0.850
x Pupil centre (mm)	0.01	1.52	0.140		
y Pupil centre (mm)	0.00	-0.36	0.720		
Apex Pachymetry (μm)	-0.36	-0.18	0.862		
Thinnest location pachymetry (μm)	1.29	0.70	0.491		
x Thinnest location (mm)	0.05	1.39	0.177		
y Thinnest location (mm)	0.04	2.11	0.045		
Corneal volume (qmm)	0.09	0.42	0.674		
Dp	-0.17	-2.13	0.043		
Dt	-0.04	-0.71	0.484		
Da	-0.13	-2.22	0.035		
Aberrations					
Coma 90° (μm)	0.00	0.17	0.868		
Coma 0° (μm)	0.02	1.08	0.291		
Trefoil (μm)	0.01	0.41	0.682		
Spherical aberration (μm)	0.00	0.01	0.996		
Density					
Density 90°	1.91	1.19	0.246		
Density 180°	1.99	1.20	0.240		
D	-0.06	-1.41	0.171	TKC (0-4)	>0.05

3.8 Results Part II (Non CXL vs. CXL)

3.8.1 Curvature data

Comparing the Non CXL and CXL groups at each of the first and second visit, the curvature based indices were found not to be significantly different ($p>0.05$, all). The data is shown in Table 3-14.

Table 3-14 Curvature data Non CXL vs. CXL at each visit

(n=36; df=70)	T-test						Mann-Whitney U test		
	Mean Non CXL	Mean CXL	t-value	p	SD Non CXL	SD CXL		p	Mann-Whitney U
Visit 1									
K max (D)	53.47	55.21	-0.88	0.381	7.79	8.97	ISV	0.173	527
K flat (D)	45.90	46.24	-0.23	0.815	5.69	6.52	IVA (mm)	0.205	535.5
K steep (D)	49.18	49.39	-0.14	0.893	6.13	6.76	KI	0.255	547
Ast (D)	3.28	2.84	0.94	0.351	2.02	1.92	CKI	0.446	580.5
Rmin (mm)	6.43	6.25	0.85	0.400	0.83	0.92			
Visit 2									
K max (D)	53.59	55.18	-0.86	0.395	7.59	8.14	ISV	0.114	507.5
K flat (D)	46.40	46.43	-0.02	0.984	6.16	6.75	IVA (mm)	0.205	535.5
K steep (D)	49.41	50.20	-0.50	0.618	6.25	7.14	KI	0.300	556
Ast (D)	3.01	3.39	-0.68	0.500	1.99	2.65	CKI	0.372	569
Rmin (mm)	6.41	6.24	0.86	0.392	0.82	0.87			

3.8.2 Elevation data

The elevation based indices showed no significant differences between the Non CXL and CXL group at each visit ($p>0.05$, all). (see Table 3-15)

Table 3-15 Elevation data Non CXL vs. CXL at each visit

(n=36; df=70)	T-test						Mann-Whitney U test		
	Mean Non CXL	Mean CXL	t-value	p	SD Non CXL	SD CXL		p	Mann-Whitney U
Visit 1 (n=36 df=70)									
BFS Front (mm)	7.47	7.47	0.04	0.967	0.50	0.67	A (0 to 4)	0.650	608
BFS Back (mm)	6.11	6.03	0.60	0.552	0.43	0.60	B (0 to 4)	0.324	569
Df	9.16	11.01	-0.97	0.334	7.47	8.70	IHA (μ m)	0.305	557
Db	7.94	10.62	-1.48	0.143	6.95	8.33	IHD (μ m)	0.173	527
Visit 2									
BFS Front (mm)	7.45	7.44	0.05	0.961	0.51	0.71	A (0 to 4)	0.830	629
BFS Back (mm)	6.12	6.03	0.77	0.446	0.41	0.59	B (0 to 4)	0.186	543
Df	9.99	10.79	-0.41	0.684	8.97	7.66	IHA (μ m)	0.411	575
Db	7.97	10.51	-1.51	0.136	6.89	7.43	IHD (μ m)	0.386	571

3.8.3 Pachymetry data

All pachymetry based indices were not significantly different between Non CXL and CXL at each visit ($p>0.05$, all). (seeTable 3-16)

Table 3-16 Pachymetry data Non CXL vs. CXL at each visit

	T-test						Mann-Whitney U test		
(n=36; df=70)	Mean Non CXL	Mean CXL	t-value	p	SD Non CXL	SD CXL		p	Mann-Whitney U
Visit 1									
Pupil centre pach. (µm)	491.44	483.19	0.59	0.559	49.77	68.07	C (0 to 4)	0.640	606.5
x Pupil centre (mm)	0.02	0.02	0.07	0.942	0.21	0.18			
y Pupil centre (mm)	0.32	0.27	0.76	0.448	0.26	0.29			
Apex Pachymetry (µm)	480.50	473.53	0.47	0.641	59.27	66.84			
Thinnest location pach. (µm)	458.33	453.19	0.31	0.760	66.78	74.89			
x Thinnest location (mm)	0.06	-0.15	1.39	0.170	0.69	0.56			
y Thinnest location (mm)	-0.72	-0.69	-0.23	0.818	0.50	0.36			
Corneal volume (qmm)	57.80	59.04	-1.18	0.243	4.11	4.81			
Dp	12.20	13.81	-0.51	0.615	13.82	13.30			
Dt	3.10	3.45	-0.43	0.669	3.10	3.72			
Da	2.92	3.07	-0.68	0.500	0.95	0.94			
Visit 2									
Pupil centre pach. (µm)	494.75	478.11	1.18	0.241	45.87	70.81	C (0 to 4)	0.414	575.5
x Pupil centre (mm)	0.01	0.02	-0.23	0.823	0.18	0.19			
y Pupil centre (mm)	0.33	0.35	-0.23	0.815	0.27	0.27			
Apex Pachymetry (µm)	483.25	466.31	1.12	0.264	54.85	71.82			
Thinnest location pach. (µm)	463.50	447.42	0.97	0.335	62.71	77.11			
x Thinnest location (mm)	0.06	-0.07	0.82	0.414	0.68	0.59			
y Thinnest location (mm)	-0.69	-0.67	-0.16	0.875	0.53	0.58			
Corneal volume (qmm)	57.91	58.45	-0.55	0.585	3.75	4.63			
Dp	11.14	14.31	-0.95	0.344	13.64	14.53			
Dt	2.86	3.81	-1.07	0.287	3.04	4.37			
Da	2.89	3.10	-0.96	0.342	0.90	0.94			

3.8.4 Aberrations

Comparing the aberrations at each visit, no significant difference was found ($p>0.05$, all). (seeTable 3-17)

Table 3-17 Aberrations Non CXL vs. CXL at each visit

(n=36; df=70)	T-test					
	Mean Non CXL	Mean CXL	t-value	p	SD Non CXL	SD CXL
Visit 1						
Coma 90° (μm)	-1.53	-1.85	1.10	0.274	1.08	1.34
Coma 0° (μm)	0.08	-0.06	0.73	0.469	0.81	0.82
Trefoil (μm)	-0.03	0.01	-0.31	0.760	0.52	0.48
Spherical aberration (μm)	-0.28	-0.35	0.41	0.686	0.70	0.78
Visit 2						
Coma 90° (μm)	-1.63	-1.79	0.55	0.583	1.14	1.37
Coma 0° (μm)	0.09	0.02	0.34	0.734	0.86	0.91
Trefoil (μm)	-0.13	-0.12	-0.03	0.974	0.60	0.45
Spherical aberration (μm)	-0.30	-0.37	0.43	0.670	0.68	0.83

3.8.5 Densitometry

For the first and second visit the density of the cornea was significantly higher in the CXL eyes compared to the non-CXL eyes ($p < 0.05$, all). (see Table 3-18) A graph is shown in Figure 3-1.

Table 3-18 Density Non CXL vs. CXL at each visit

(n=36; df=70)	T-test					
	Mean Non CXL	Mean CXL	t-value	p	SD Non CXL	SD CXL
Visit 1						
Density 90°	36.08	42.08	-2.20	0.031	9.05	13.67
Density 180°	36.63	43.08	-2.32	0.023	9.48	13.71
Visit 2						
Density 90°	37.57	47.81	-2.65	0.010	10.07	20.92
Density 180°	36.95	45.47	-2.18	0.032	11.70	20.28

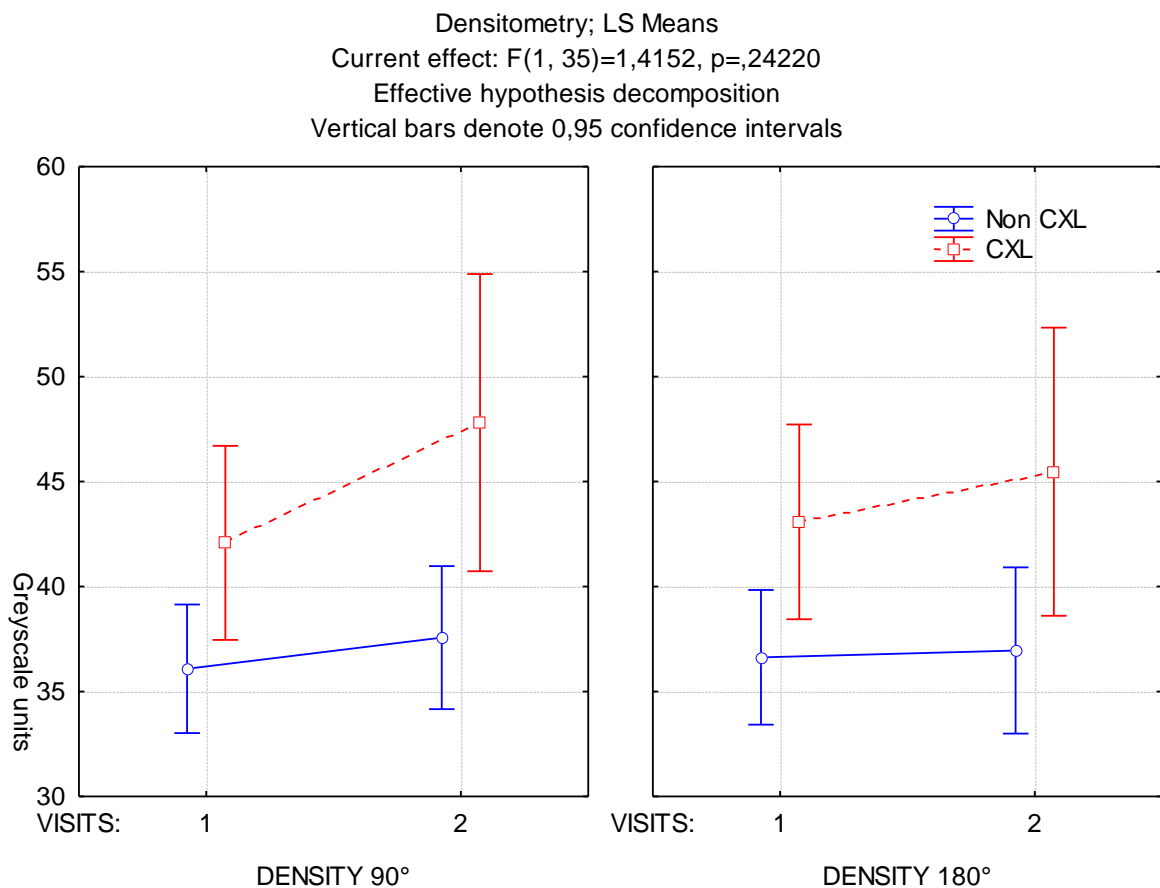


Figure 3-1 Densitometry Non CXL vs. CXL Visit 1 vs. Visit 2

3.8.6 Final D value and TKC

There was no significant difference found for the D value or TKC for each visit ($p>0.05$, all) but the CXL group had higher values compared to the non-CXL group for both indices. (see Table 3-19) There was no significant correlation between the TKC and age ($p>0.05$).

Table 3-19 D and TKC Non CXL vs. CXL at each visit

(n=36; df=70)	T-test						Mann-Whitney U test		
	Mean Non CXL	Mean CXL	t-value	p	SD Non CXL	SD CXL		p	Mann-Whitney U
Visit 1									
D	9.24	10.42	-0.78	0.436	6.55	6.17	TKC (0-4)	0.174	529
Visit 2									
D	9.12	10.46	-0.89	0.377	6.65	6.11	TKC (0-4)	0.227	542.5

3.9 Results Part III (comparing visits by CXL)

3.9.1 Curvature data

Comparing the visits within the Non CXL group, K flat was found to be significantly steeper from visit 1 to 2 ($p=0.021$). (see Table 3-20) In the CXL group there was a difference from the first to the second visit for K steep ($p=0.028$) as it also steepened and CKI increased ($p=0.046$). (see Table 3-21) A graph of the curvature data can be found in Figure 3-2.

Table 3-20 Curvature data Non CXL comparing each visit

Non CXL n=36	T test				Wilcoxon Test			
	Mean (\pm SD) Visit 1	Mean (\pm SD) Visit 2	t-value	p		Mean (\pm SD) Visit 1	Mean (\pm SD) Visit 2	p
K max (D)	53.47 (\pm 7.79)	53.59 (\pm 7.59)	-0.39	0.695	ISV	75.97 (\pm 38.45)	79.08 (\pm 42.91)	0.564
K flat (D)	45.90 (\pm 5.69)	46.40 (\pm 6.16)	-2.42	0.021	IVA (mm)	0.77 (\pm 0.41)	0.78 (\pm 0.44)	0.876
K steep (D)	49.18 (\pm 6.13)	49.41 (\pm 6.25)	-0.92	0.364	KI	1.20 (\pm 0.12)	1.20 (\pm 0.13)	0.830
Ast (D)	3.28 (\pm 2.02)	3.01 (\pm 1.99)	1.59	0.121	CKI	1.04 (\pm 0.05)	1.05 (\pm 0.05)	0.312
Rmin (mm)	6.43 (\pm 0.83)	6.41 (\pm 0.82)	0.63	0.532				

Table 3-21 Curvature data CXL comparing each visit

CXL n=36	T test				Wilcoxon Test			
	Mean (\pm SD) Visit 1	Mean (\pm SD) Visit 2	t-value	p		Mean (\pm SD) Visit 1	Mean (\pm SD) Visit 2	p
K max (D)	55.21 (\pm 8.97)	55.18 (\pm 8.14)	0.08	0.938	ISV	91.19 (\pm 40.32)	93.83 (\pm 39.69)	0.130
K flat (D)	46.24 (\pm 6.52)	46.43 (\pm 6.75)	-0.81	0.424	IVA (mm)	0.94 (\pm 0.47)	5.25 (\pm 26.02)	0.981
K steep (D)	49.39 (\pm 6.76)	50.20 (\pm 7.14)	-2.29	0.028	KI	1.24 (\pm 0.15)	1.32 (\pm 0.56)	0.820
Ast (D)	2.84 (\pm 1.92)	3.39 (\pm 2.65)	-1.40	0.171	CKI	1.05 (\pm 0.06)	1.06 (\pm 0.06)	0.046
Rmin (mm)	6.25 (\pm 0.92)	6.24 (\pm 0.87)	0.38	0.706				

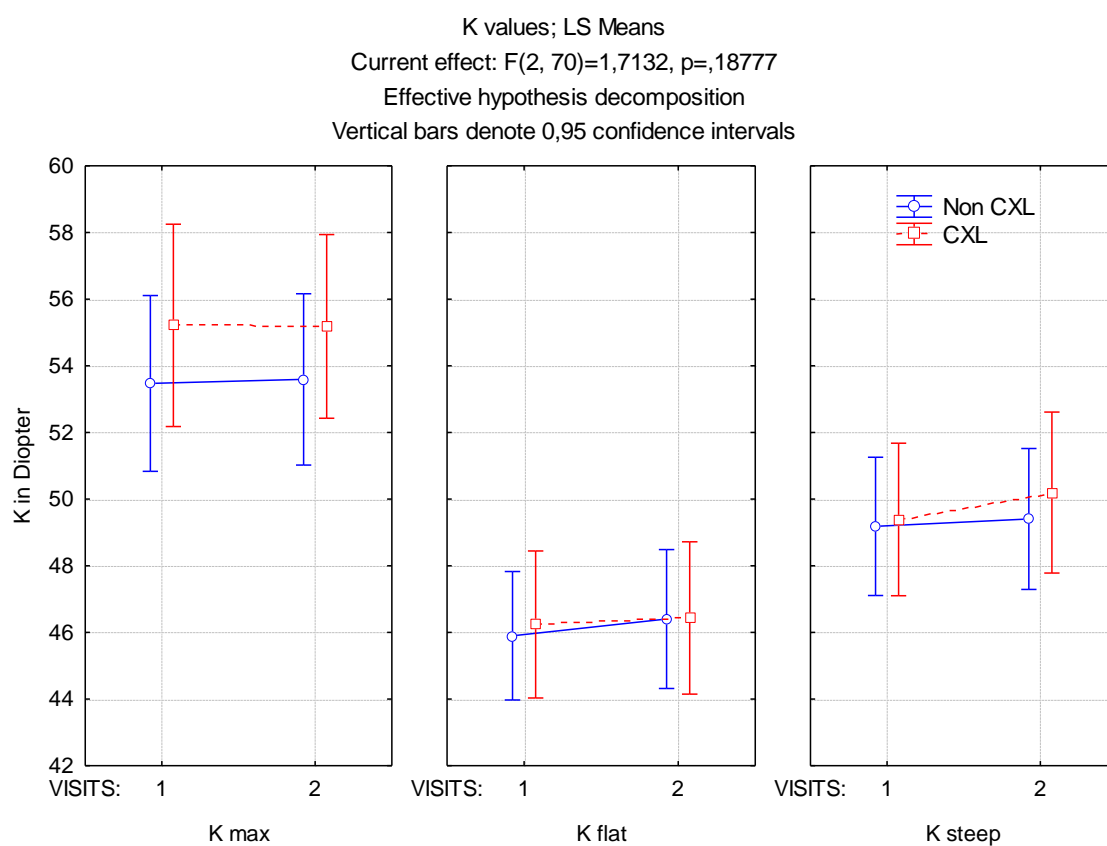


Figure 3-2 K values Non CXL vs. CXL Visit 1 vs. Visit 2

3.9.2 Elevation data

For both groups IHD was significantly different between each visit (Non CXL: $p=0.008$ and CXL: $p=0.046$). (see Table 3-22 and Table 3-23) Figure 3-3 shows the increases in IHD for both groups from visit 1 to visit 2.

Table 3-22 Elevation data Non CXL comparing visits

Non CXL n=36	T test				Wilcoxon Test			
	Mean (\pm SD) Visit 1	Mean (\pm SD) Visit 2	t-value	p		Mean (\pm SD) Visit 1	Mean (\pm SD) Visit 2	p
BFS Front (mm)	7.47 (\pm 0.50)	7.45 (\pm 0.51)	1.77	0.086	A (0 to 4)	2.02 (\pm 1.45)	2.09 (\pm 1.44)	0.095
BFS Back (mm)	6.11 (\pm 0.43)	6.12 (\pm 0.41)	-0.42	0.678	B (0 to 4)	2.87 (\pm 1.39)	2.94 (\pm 1.38)	0.808
Df	9.16 (\pm 7.47)	9.99 (\pm 8.97)	-1.18	0.247	IHA (μ m)	22.60 (\pm 25.25)	29.25 (\pm 22.70)	0.145
Db	7.94 (\pm 6.95)	7.97 (\pm 6.89)	-0.06	0.953	IHD (μ m)	0.09 (\pm 0.06)	0.10 (\pm 0.06)	0.008

Table 3-23 Elevation data CXL comparing visits

CXL n=36	T test				Wilcoxon Test			
	Mean (\pm SD) Visit 1	Mean (\pm SD) Visit 2	t-value	p		Mean (\pm SD) Visit 1	Mean (\pm SD) Visit 2	p
BFS Front (mm)	7.47 (\pm 0.67)	7.44 (\pm 0.71)	0.74	0.467	A (0 to 4)	2.17 (\pm 1.49)	2.16 (\pm 1.49)	0.870
BFS Back (mm)	6.03 (\pm 0.60)	6.03 (\pm 0.59)	0.17	0.865	B (0 to 4)	3.16 (\pm 1.49)	3.16 (\pm 1.48)	0.695
Df	11.01 (\pm 8.70)	10.79 (\pm 7.66)	0.35	0.728	IHA (μ m)	26.98 (\pm 23.86)	27.32 (\pm 25.89)	0.891
Db	10.62 (\pm 8.33)	10.51 (\pm 7.43)	0.21	0.837	IHD (μ m)	0.10 (\pm 0.06)	0.11 (\pm 0.06)	0.046

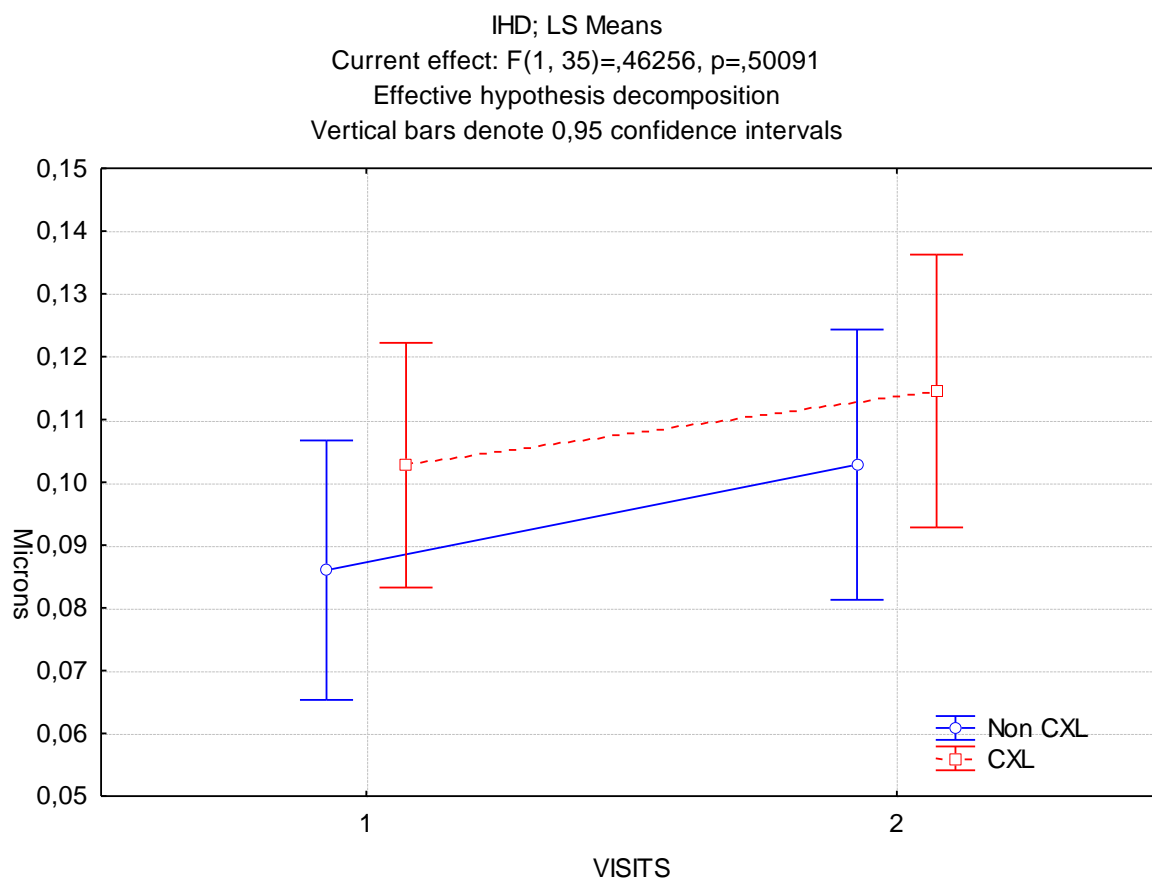


Figure 3-3 IHD Non CXL vs. CXL Visit 1 vs. Visit 2

3.9.3 Pachymetry data

Comparing the visits within the Non CXL group, the pachymetry at the thinnest point significantly increased ($p=0.02$) and Dt was reduced ($p=0.027$). (see Table 3-24) In the CXL group the y location of the pupil centre changed significantly ($p=0.024$). (see Table 3-25)

Table 3-24 Pachymetry data Non CXL comparing visits

Non CXL n=36	T test				Wilcoxon Test			
	Mean (\pm SD) Visit 1	Mean (\pm SD) Visit 2	t-value	p		Mean (\pm SD) Visit 1	Mean (\pm SD) Visit 2	p
Pupil centre pach. (μ m)	491.44 (\pm 49.77)	494.75 (\pm 45.87)	-1.56	0.127	C (0 to 4)	1.74 (\pm 1.11)	1.65 (\pm 1.03)	0.073
x Pupil centre (mm)	0.02 (\pm 0.21)	0.01 (\pm 0.18)	0.63	0.534				
y Pupil centre (mm)	0.32 (\pm 0.26)	0.33 (\pm 0.27)	-0.64	0.527				
Apex Pachymetry (μ m)	480.50 (\pm 59.27)	483.25 (\pm 54.85)	-1.25	0.220				
Thinnest loc. pach. (μ m)	458.33 (\pm 66.78)	463.50 (\pm 62.71)	-2.43	0.020				
x Thinnest loc. (mm)	0.06 (\pm 0.69)	0.06 (\pm 0.68)	0.01	0.993				
y Thinnest loc. (mm)	-0.72 (\pm 0.50)	-0.69 (\pm 0.53)	-0.70	0.489				
Corneal volume (qmm)	57.80 (\pm 4.11)	57.91 (\pm 3.75)	-0.45	0.655				
Dp	12.20 (\pm 13.82)	11.14 (\pm 13.64)	1.05	0.291				
Dt	3.10 (\pm 3.10)	2.86 (\pm 3.04)	0.24	0.027				
Da	2.92 (\pm 0.95)	2.89 (\pm 0.90)	0.03	0.588				

Table 3-25 Pachymetry data CXL comparing visits

CXL n=36	T test				Wilcoxon Test			
	Mean (\pm SD) Visit 1	Mean (\pm SD) Visit 2	t-value	p		Mean (\pm SD) Visit 1	Mean (\pm SD) Visit 2	p
Pupil centre pach. (μ m)	483.19 (\pm 68.07)	478.11 (\pm 70.81)	1.16	0.254	C (0 to 4)	1.85 (\pm 1.16)	1.89 (\pm 1.20)	0.264
x Pupil centre (mm)	0.02 (\pm 0.18)	0.02 (\pm 0.19)	-0.28	0.783				
y Pupil centre (mm)	0.27 (\pm 0.29)	0.35 (\pm 0.27)	-2.36	0.024				
Apex Pachymetry (μ m)	473.53 (\pm 66.84)	466.31 (\pm 71.82)	1.89	0.067				
Thinnest loc. pach. (μ m)	453.19 (\pm 74.89)	447.42 (\pm 77.11)	1.36	0.181				
x Thinnest loc. (mm)	-0.15 (\pm 0.56)	-0.07 (\pm 0.59)	-1.18	0.246				
y Thinnest loc. (mm)	-0.69 (\pm 0.36)	-0.67 (\pm 0.58)	-0.29	0.775				
Corneal volume (qmm)	59.04 (\pm 4.81)	58.45 (\pm 4.63)	1.47	0.150				
Dp	13.81 (\pm 13.30)	14.31 (\pm 14.53)	-0.37	0.711				
Dt	3.45 (\pm 3.72)	3.81 (\pm 4.37)	-1.43	0.162				
Da	3.07 (\pm 0.94)	3.10 (\pm 0.94)	-0.62	0.542				

3.9.4 Aberrations

In the both groups there was no significant difference found ($p>0.05$, all). (see Table 3-26 and Table 3-27)

Table 3-26 Aberrations Non CXL comparing visits

Non CXL	T test			
n=36	Mean (\pm SD) Visit 1	Mean (\pm SD) Visit 2	t-value	p
Coma 90° (μ m)	-1.53 (\pm 1.08)	-1.63 (\pm 1.14)	-0.50	0.622
Coma 0° (μ m)	0.08 (\pm 0.81)	0.09 (\pm 0.86)	-1.22	0.229
Trefoil (μ m)	-0.03 (\pm 0.52)	-0.13 (\pm 0.60)	1.44	0.159
Spherical aberration (μ m)	-0.28 (\pm 0.70)	-0.30 (\pm 0.68)	0.37	0.713

Table 3-27 Aberrations CXL comparing visits

CXL	T test			
n=36	Mean (\pm SD) Visit 1	Mean (\pm SD) Visit 2	t-value	p
Coma 90° (μ m)	-1.85 (\pm 1.34)	-1.79 (\pm 1.37)	-0.50	0.622
Coma 0° (μ m)	-0.06 (\pm 0.82)	0.02 (\pm 0.91)	-1.22	0.229
Trefoil (μ m)	0.01 (\pm 0.48)	-0.12 (\pm 0.45)	1.44	0.159
Spherical aberration (μ m)	-0.35 (\pm 0.78)	-0.37 (\pm 0.83)	0.37	0.713

3.9.5 Densitometry

Both groups showed no significant difference in Density ($p>0.05$, all) although the CXL group showed an increase in density comparing visits. (see Table 3-28 and Table 3-29)

Table 3-28 Density Non CXL comparing visits

Non CXL	T test			
n=36	Mean (\pm SD) Visit 1	Mean (\pm SD) Visit 2	t-value	p
Density 90°	36.08 (\pm 9.05)	37.57 (\pm 10.07)	-0.80	0.431
Density 180°	36.63 (\pm 9.48)	36.95 (\pm 11.70)	-0.15	0.881

Table 3-29 Density CXL comparing visits

CXL	T test			
n=36	Mean (\pm SD) Visit 1	Mean (\pm SD) Visit 2	t-value	p
Density 90°	42.08 (\pm 13.67)	47.81 (\pm 20.92)	-1.77	0.086
Density 180°	43.08 (\pm 13.71)	45.47 (\pm 20.28)	-0.75	0.458

3.9.6 Final D value and TKC

There was no significant difference in the both groups ($p > 0.05$, all) comparing visits. (see Table 3-30 and Table 3-31) For the CXL group, despite not being significant, there was an increase in the D value and TKC.

Table 3-30 D and TKC Non CXL comparing visits

Non CXL	T test				Wilcoxon Test			
n=36	Mean (\pm SD) Visit 1	Mean (\pm SD) Visit 2	t-value	p		Mean (\pm SD) Visit 1	Mean (\pm SD) Visit 2	p
D	9.24 (\pm 6.55)	9.12 (\pm 6.65)	0.13	0.615	TKC (0-4)	1.93 (\pm 1.06)	2.03 (\pm 1.07)	0.622

Table 3-31 D and TKC CXL comparing visits

CXL	T test				Wilcoxon Test			
n=36	Mean (\pm SD) Visit 1	Mean (\pm SD) Visit 2	t-value	p		Mean (\pm SD) Visit 1	Mean (\pm SD) Visit 2	p
D	10.42 (\pm 1.03)	10.46 (\pm 6.11)	-0.11	0.914	TKC (0-4)	2.25 (\pm 1.08)	2.58 (\pm 0.88)	0.313

3.10 Discussion

This study was a retrospective chart review examining a number of corneal factors that could determine diagnosis to differentiate between normal and KC and monitor the progression in those who were diagnosed with KC. The data were collected at two visit points that were separated by approximately 1.5 years. There was a difference in follow up time when the KC population was divided into two groups, those with and those without corneal cross-linking. The CXL group was followed up more frequently and closely compared to the Non CXL group. Despite the fact that CXL is normally performed on a younger and more progressive group of individuals (67) there was not a significant difference in ages in our study compared to the non-CXL group (n=36). There was a significant difference in age comparing Non CXL (older) when matched with the control group (n=28) but no difference between CXL and control. The CXL group was younger as expected and better matched to the control group.

The population was further sub-divided into two groups as to whether they had atopic disease (and no CXL) associated with KC or not, in order to differentiate results at each visit. Comparing visit 1 to visit 2 the atopic group showed no differences in the indices examined indicating that despite eye rubbing a direct consequence (86) or diagnostic factor (87, 88) related to KC is less influential on the progression of the disease.

As a diagnostic tool the Pentacam HR® has a variety of curvature, elevation and pachymetric factors and indices, based on those factors, which differentiate KC from the normal eye. (89) In this study all of the factors and indices examined showed a significant difference at each visit when compared to normals. When comparing CXL to non-CXL the factor that predominated was the Densitometry measure which was increased in the CXL group, as there were no differences in the curvature, elevation or pachymetric data at each visit. Although not statistically different there was a slight increase in Densitometry from visit 1 to visit 2 for the CXL group.

The densitometry values were higher in this study for all groups including normals. The ranges of the values for the CXL group were from the mid-twenties to the mid-eighties due to the range of time of when the CXL was performed. It is therefore difficult to compare these results to Greenstein et al (90) where they found 21.4 ± 3.9 in KC eyes with CXL after 3 months postoperatively, a much shorter timeframe. Other studies show that corneal haze might occur after CXL and that it declines over the first year but there is little evidence that there are any changes beyond the first year. (90, 91)

There is also little evidence that the Pentacam HR® is useful to monitor progression of KC or to detect the effects of corneal cross-linking on the progression of KC. This study has found some factors and indices that may be useful to do this, as a practitioner would be over-whelmed when examining the Pentacam HR® data due to its large volume.

The curvature based data that best described progression was the FlatK for the non-CXL group and the SteepK and CKI for the CXL group. This is in support of other papers that have shown that the K readings from a tomographer based on thousands of points is a reliable and repeatable measure to detect progression. (92, 93) The CKI values in this study are in the range of the study of Hashemi et al (89) as they found a CKI of 1.03-1.12 for keratoconic eyes and comparable to the result of a mean CKI of 1.06 ± 0.07 found in the study of Kanellopoulus et al. (82) The elevation based data that best described progression for both groups was the IHD (index of height decentration). The IHD has been confirmed to be an indicator for KC detection by others (89, 94) and the study of Kanellopoulos et al supports the result of IHD as a progression criteria with a mean IHD of 0.091 ± 0.054 for KC which is comparable to this study's findings. (82) The results of this study also fall in the range of the results of the study of Hashemi et al (89) as they found an IHD of 0.051-0.122. On the other hand, it should be considered that in this study also the control group showed a change in the IHD (without outliers removed) which could be reflective of the sample of convenience that was chosen.

As for the pachymetric based data, the thickness at the thinnest point and Dt (index based on thickness) were showing a statistically significant increase in thickness within the non-CXL group by ≈ 5 microns which may not be clinically relevant and a non-significant decrease in thickness with the CXL group. As the non CXL group was slightly older, then they may not have significantly progressed between the two visits. The thickness based indices are dependent on a change in thickness from the centre to the periphery of the cornea where the accuracy of the instrument declines (5, 78) It is commonly known that KC progression can be measured by monitoring corneal thickness. (25) Some studies showed a slight increase by 2-3 microns or stabilization of the corneal thickness in non-progressive eyes. (95, 96) The change in the y location of the pupil centre relative to the apex based on the location of highest elevation, when examining the CXL data was most significant as it became more decentred. The x location was closer to the apex by the second visit, but not significantly for the CXL group and no change for the non-CXL group. Recent literature does indicate that the location of the cone does change after CXL, but the location is described as being more centred relative to the apex, especially when the cone is more inferiorly displaced. (97, 98)

3.11 Conclusion

In conclusion, this review on a limited number of KC participants has demonstrated that the Pentacam HR® and its factors and indices can be useful in detecting the progression of KC with and without CXL and atopic disease, in addition, to their use in early diagnosis of KC when compare to controls.

4 Literature Cited

1. Barboni P, Savini G, Carbonelli M, Hoffer KJ. Agreement between Pentacam and videokeratography in corneal power assessment. *Journal of Refractive Surgery* 2009; 25(6):534–8.
2. Guillon M, Lydon DPM, Wilson C. Corneal topography: a clinical model. *Ophthalmic and Physiological Optics* 1986; 6(1):47–56.
3. Rüfer F, Schröder A, Erb C. White-to-white corneal diameter: normal values in healthy humans obtained with the Orbscan II topography system. *Cornea* 2005; 24(3):259–61.
4. Kiely PM, Smith G, Carney LG. The mean shape of the human cornea. *Optica Acta: International Journal of Optics* 1982; 29(8):1027–40.
5. Khoramnia R, Rabsilber TM, Auffarth GU. Central and peripheral pachymetry measurements according to age using the Pentacam rotating Scheimpflug camera. *Journal of Cataract & Refractive Surgery* 2007; 33(5):830–6.
6. Sin S, Simpson TL. The repeatability of corneal and corneal epithelial thickness measurements using optical coherence tomography. *Optometry Vision Sci.* 2006; 83(6):360–5.
7. Eghbali F, Yeung KK, Maloney RK. Topographic determination of corneal asphericity and its lack of effect on the refractive outcome of radial keratotomy. *Am. J. Ophthalmol.* 1995; 119(3):275–80.
8. Fledelius HC, Stubgaard M. Changes in refraction and corneal curvature during growth and adult life: A cross-sectional study. *Acta Ophthalmol.* 1986; 64(5):487–91.
9. Dubbelman M, Sicam V, van der Heijde GL. The shape of the anterior and posterior surface of the aging human cornea. *Vision Res.* 2006; 46(6-7):993–1001.
10. Eysteinnsson T, Jonasson F, Sasaki H, Arnarsson A, Sverrisson T, Sasaki K et al. Central corneal thickness, radius of the corneal curvature and intraocular pressure in

normal subjects using non-contact techniques: Reykjavik Eye Study. *Acta Ophthalmol. Scand.* 2002; 80(1):11–5.

11. Ferrer-Blasco T, González-Méijome JM, Montés-Micó R. Age-related changes in the human visual system and prevalence of refractive conditions in patients attending an eye clinic. *Journal of Cataract & Refractive Surgery* 2008; 34(3):424–32.

12. Goto T, Klyce SD, Zheng X, Maeda N, Kuroda T, Ide C. Gender-and age-related differences in corneal topography. *Cornea* 2001; 20(3):270–6.

13. DelMonte DW, Kim T. Anatomy and physiology of the cornea. *Journal of Cataract & Refractive Surgery* 2011; 37(3):588–98.

14. Farjo A, McDermott M, Soong HK. Corneal anatomy, physiology, and wound healing. *Ophthalmology* 2009; 44(2):203–8.

15. Dua HS, Azuara-Blanco A. Limbal stem cells of the corneal epithelium. *Surv. Ophthalmol.* 2000; 44(5):415–25.

16. Maurice DM. The structure and transparency of the cornea. *J. Physiol. (Lond.)* 1957; 136(2):263–86.

17. West-Mays JA, Dwivedi DJ. The keratocyte: corneal stromal cell with variable repair phenotypes. *Int. J. Biochem. Cell Biol.* 2006; 38(10):1625–31.

18. Johnson DH, Bourne WM, Campbell RJ. The ultrastructure of Descemet's membrane: I. Changes with age in normal corneas. *Arch. Ophthalmol.* 1982; 100(12):1942–7.

19. RABINOWITZ YS. Keratoconus. *Surv. Ophthalmol.* 1998; 42(4):297–319.

20. Kennedy RH, Bourne WM, Dyer JA. A 48-year clinical and epidemiologic study of keratoconus. *Am. J. Ophthalmol.* 1986; 101(3):267–73.

21. Gorskova EN, Sevost'ianov EN. Epidemiology of keratoconus in the Urals. *Vestn. Oftalmol.* 1998; 114(4):38–40.

22. Jonas JB, Nangia V, Matin A, Kulkarni M, Bhojwani K. Prevalence and associations of keratoconus in rural maharashtra in central India: the central India eye and medical study. *Am. J. Ophthalmol.* 2009; 148(5):760–5.
23. Pearson AR, Soneji B, Sarvananthan N, Sandford-Smith JH. Does ethnic origin influence the incidence or severity of keratoconus? *Eye* 2000; 14(4):625.
24. Georgiou T, Funnell CL, Cassels-Brown A, O'Connor R. Influence of ethnic origin on the incidence of keratoconus and associated atopic disease in Asians and white patients. *Eye* 2004; 18(4):379.
25. Gomes JA, Tan D, Rapuano CJ, Belin MW, Ambrosio, R. ,Jr, Guell JL et al. Global consensus on keratoconus and ectatic diseases. *Cornea* 2015; 34(4):359–69.
26. Rabinowitz YS, Garbus J, McDonnell PJ. Computer-assisted corneal topography in family members of patients with keratoconus. *Arch. Ophthalmol.* 1990; 108(3):365–71.
27. Hammerstein W. Zur genetik des keratoconus. *Albrecht von Graefes Archiv für klinische und experimentelle Ophthalmologie* 1974; 190(4):293–308.
28. AUSTIN MG, SCHAEFER RF. Marfan's syndrome, with unusual blood vessel manifestations. *AMA Arch. Pathol.* 1957; 64(2):205–9.
29. Kenney MC, Brown DJ. The cascade hypothesis of keratoconus. *Contact lens and anterior eye* 2003; 26(3):139–46.
30. Buddi R, Lin B, Atilano SR, Zorapapel NC, Kenney MC, Brown DJ. Evidence of oxidative stress in human corneal diseases. *Journal of Histochemistry & Cytochemistry* 2002; 50(3):341–51.
31. Weed KH, MacEwen CJ, Giles T, Low J, McGhee CNJ. The Dundee University Scottish Keratoconus study: demographics, corneal signs, associated diseases, and eye rubbing. *Eye* 2008; 22(4):534.
32. Bawazeer AM, Hodge WG, Lorimer B. Atopy and keratoconus: a multivariate analysis. *Br. J. Ophthalmol.* 2000; 84(8):834–6.

33. Balasubramanian SA, Pye DC, Willcox MDP. Effects of eye rubbing on the levels of protease, protease activity and cytokines in tears: relevance in keratoconus. *Clinical and Experimental Optometry* 2013; 96(2):214–8.
34. Romano V, Vinciguerra R, Arbabi EM, Hicks N, Rosetta P, Vinciguerra P et al. Progression of keratoconus in patients while awaiting corneal cross-linking: a prospective clinical study. *Journal of Refractive Surgery* 2018; 34(3):177–80.
35. Reeves SW, Stinnett S, Adelman RA, Afshari NA. Risk factors for progression to penetrating keratoplasty in patients with keratoconus. *Am. J. Ophthalmol.* 2005; 140(4):607. e1-607. e6.
36. Shetty R, Kaweri L, Pahuja N, Nagaraja H, Wadia K, Jayadev C et al. Current review and a simplified "five-point management algorithm" for keratoconus. *Indian J. Ophthalmol.* 2015; 63(1):46–53.
37. Sherwin T, Brookes NH. Morphological changes in keratoconus: pathology or pathogenesis. *Clin. Experiment. Ophthalmol.* 2004; 32(2):211–7.
38. Fernandes BF, Logan P, Zajdenweber ME, Santos LN, Cheema DP, Burnier Jr MN. Histopathological study of 49 cases of keratoconus. *Pathology* 2008; 40(6):623–6.
39. KIM W-J, RABINOWITZ YS, MEISLER DM, WILSON SE. Keratocyte apoptosis associated with keratoconus. *Exp. Eye Res.* 1999; 69(5):475–81.
40. Somodi S, Hahnel C, Slowik C, Richter A, Weiss DG, Guthoff R. Confocal in vivo microscopy and confocal laser-scanning fluorescence microscopy in keratoconus. *Ger. J. Ophthalmol.* 1996; 5(6):518–25.
41. Scroggs MW, Proia AD. Histopathological variation in keratoconus. *Cornea* 1992; 11(6):553–9.
42. Kenney MC, Nesburn AB, Burgeson RE, Butkowski RJ, Ljubimov AV. Abnormalities of the extracellular matrix in keratoconus corneas. *Cornea* 1997; 16(3):345–51.

43. Takahashi A, Nakayasu K, Okisaka S, Kanai A. Quantitative analysis of collagen fiber in keratoconus. *Nippon Ganka Gakkai Zasshi* 1990; 94(11):1068–73.
44. Mathew JH, Goosey JD, Bergmanson JPG. Quantified histopathology of the keratoconic cornea. *Optometry and vision science: official publication of the American Academy of Optometry* 2011; 88(8):988.
45. Jongebloed WL, Dijk F, Worst JGF. Keratoconus morphology and cell dystrophy: a SEM study. *Documenta ophthalmologica* 1989; 72(3-4):403–9.
46. Kaldawy RM, Wagner J, Ching S, Seigel GM. Evidence of apoptotic cell death in keratoconus. *Cornea* 2002; 21(2):206–9.
47. Krachmer JH, Feder RS, Belin MW. Keratoconus and related noninflammatory corneal thinning disorders. *Surv. Ophthalmol.* 1984; 28(4):293–322.
48. Hosseini SMA, Mohidin N, Abolbashari F, Mohd-Ali B, Santhirathelagan CT. Corneal thickness and volume in subclinical and clinical keratoconus. *Int. Ophthalmol.* 2013; 33(2):139–45.
49. Mannion LS, Tromans C, O'Donnell C. Reduction in corneal volume with severity of keratoconus. *Curr. Eye Res.* 2011; 36(6):522–7.
50. Duke-Elder SL. *System of ophthalmology/VolIII: diseases of the outer eye part 2* 1965.
51. Burns DM, Johnston FM, Frazer DG, Patterson C, Jackson AJ. Keratoconus: an analysis of corneal asymmetry. *Br. J. Ophthalmol.* 2004; 88(10):1252–5.
52. Perry HD, Buxton JN, Fine BS. Round and oval cones in keratoconus. *Ophthalmology* 1980; 87(9):905–9.
53. Barr JT, Wilson BS, Gordon MO, Rah MJ, Riley C, Kollbaum PS et al. Estimation of the incidence and factors predictive of corneal scarring in the Collaborative Longitudinal Evaluation of Keratoconus (CLEK) Study. *Cornea* 2006; 25(1):16–25.
54. Alió JL, Shabayek MH. Corneal higher order aberrations: a method to grade keratoconus. *Journal of Refractive Surgery* 2006; 22(6):539–45.

55. Aksoy S, Akkaya S, Ozkurt Y, Kurna S, Acikalin B, Sengor T. Topography and Higher Order Corneal Aberrations of the Fellow Eye in Unilateral Keratoconus. *Turk. J. Ophthalmol.* 2017; 47(5):249–54.
56. Mrazovac D, Barisic Kutija M, Vidas S, Kuzman T, Petricek I, Jandrokovic S et al. Contact lenses as the best conservative treatment of newly diagnosed keratoconus--epidemiological retrospective study. *Coll. Antropol.* 2014; 38(4):1115–8.
57. Leung KKY. RGP fitting philosophies for keratoconus. *Clinical and Experimental Optometry* 1999; 82(6):230–5.
58. González-Méijome JM, Jorge J, Almeida JB de, Parafita MA. Soft contact lenses for keratoconus: case report. *Eye Contact Lens* 2006; 32(3):143–7.
59. Rathi VM, Mandathara PS, Dumpati S. Contact lens in keratoconus. *Indian J. Ophthalmol.* 2013; 61(8):410–5.
60. Moffatt SL, Cartwright VA, Stumpf TH. Centennial review of corneal transplantation. *Clin. Experiment. Ophthalmol.* 2005; 33(6):642–57.
61. Wollensak G, Spoerl E, Seiler T. Riboflavin/ultraviolet-A-induced collagen crosslinking for the treatment of keratoconus. *Am. J. Ophthalmol.* 2003; 135(5):620–7.
62. O'Brart DPS, Patel P, Lascaratos G, Wagh VK, Tam C, Lee J et al. Corneal cross-linking to halt the progression of keratoconus and corneal ectasia: seven-year follow-up. *Am. J. Ophthalmol.* 2015; 160(6):1154–63.
63. Chatzis N, Hafezi F. Progression of keratoconus and efficacy of pediatric [corrected] corneal collagen cross-linking in children and adolescents. *J. Refract. Surg.* 2012; 28(11):753–8.
64. Raiskup-Wolf F, Hoyer A, Spoerl E, Pillunat LE. Collagen crosslinking with riboflavin and ultraviolet-A light in keratoconus: long-term results. *Journal of Cataract & Refractive Surgery* 2008; 34(5):796–801.
65. Wollensak G. Crosslinking treatment of progressive keratoconus: new hope. *Curr. Opin. Ophthalmol.* 2006; 17(4):356–60.

66. Wollensak G, Wilsch M, Spoerl E, Seiler T. Collagen fiber diameter in the rabbit cornea after collagen crosslinking by riboflavin/UVA. *Cornea* 2004; 23(5):503–7.
67. Randleman JB, Khandelwal SS, Hafezi F. Corneal cross-linking. *Surv. Ophthalmol.* 2015; 60(6):509–23.
68. Randleman JB, Russell B, Ward MA, Thompson KP, Stulting RD. Risk factors and prognosis for corneal ectasia after LASIK. *Ophthalmology* 2003; 110(2):267–75.
69. Jinabhai A, Radhakrishnan H, O'Donnell C. Pellucid corneal marginal degeneration: A review. *Contact lens and anterior eye* 2011; 34(2):56–63.
70. Srinivasan S, Murphy CC, Fisher AC, Freeman LB, Kaye SB. Terrien marginal degeneration presenting with spontaneous corneal perforation. *Cornea* 2006; 25(8):977–80.
71. Mejía-Barbosa Y, Malacara-Hernández D. A review of methods for measuring corneal topography. *Optometry Vision Sci.* 2001; 78(4):240–53.
72. Brody J, Waller S, Wagoner M. Corneal topography: history, technique, and clinical uses. *Int. Ophthalmol. Clin.* 1994; 34(3):197–207.
73. Belin MW, Khachikian SS. An introduction to understanding elevation-based topography: how elevation data are displayed—a review. *Clin. Experiment. Ophthalmol.* 2009; 37(1):14–29.
74. Best N, Drury L, Wolffsohn JS. Clinical evaluation of the Oculus Keratograph. *Contact lens and anterior eye* 2012; 35(4):171–4.
75. Ambrósio R, Belin MW. Imaging of the cornea: topography vs tomography. *Journal of Refractive Surgery* 2010; 26(11):847–9.
76. Oliveira CM, Ribeiro C, Franco S. Corneal imaging with slit-scanning and Scheimpflug imaging techniques. *Clinical and Experimental Optometry* 2011; 94(1):33–42.
77. Oculus Optikgeräte GmbH. Pentacam HR® Interpretation Guide. 3rd edition. Wetzlar, Germany.

78. Otchere H, Sorbara L. Repeatability of topographic corneal thickness in keratoconus comparing Visante™ OCT and Oculus Pentacam HR® topographer. *Contact lens and anterior eye* 2017; 40(4):217–23.
79. Manual PU. Wetzlar. Germany: Oculus Optikgerate GmBH 2008.
80. Otri AM, Fares U, Al-Aqaba MA, Dua HS. Corneal densitometry as an indicator of corneal health. *Ophthalmology* 2012; 119(3):501–8.
81. Dhubhghaill SN, Rozema JJ, Jongenelen S, Hidalgo IR, Zakaria N, Tassignon M-J. Normative values for corneal densitometry analysis by Scheimpflug optical assessment. *Invest. Ophthalmol. Vis. Sci.* 2014; 55(1):162–8.
82. Kanellopoulos AJ, Asimellis G. Revisiting keratoconus diagnosis and progression classification based on evaluation of corneal asymmetry indices, derived from Scheimpflug imaging in keratoconic and suspect cases. *Clin. Ophthalmol.* 2013; 7:1539–48.
83. Krumeich JH, Daniel J, Knülle A. Live-epikeratophakia for keratoconus. *Journal of Cataract & Refractive Surgery* 1998; 24(4):456–63.
84. Belin MW, Steinmueller M. The brains behind the BAD. *Ophthalmology Times Europe* 2009.
85. Belin MW, Duncan JK. Keratoconus: The ABCD Grading System. *Klin. Monbl Augenheilkd.* 2016; 233(6):701–7.
86. McMonnies CW. Mechanisms of rubbing-related corneal trauma in keratoconus. *Cornea* 2009; 28(6):607–15.
87. Edwards M, McGhee CNJ, Dean S. The genetics of keratoconus. *Clin. Experiment. Ophthalmol.* 2001; 29(6):345–51.
88. Kaiserman I, Sella S. Chronic Ocular Inflammation and Keratoconus. In: *Controversies in the Management of Keratoconus*: Springer; 2019. p. 17–27.
89. Hashemi H, Beiranvand A, Yekta A, Maleki A, Yazdani N, Khabazkhoob M. Pentacam top indices for diagnosing subclinical and definite keratoconus. *Journal of current ophthalmology* 2016; 28(1):21–6.

90. Greenstein SA, Fry KL, Bhatt J, Hersh PS. Natural history of corneal haze after collagen crosslinking for keratoconus and corneal ectasia: Scheimpflug and biomicroscopic analysis. *Journal of Cataract & Refractive Surgery* 2010; 36(12):2105–14.
91. Raiskup F, Hoyer A, Spoerl E. Permanent corneal haze after riboflavin-UVA-induced cross-linking in keratoconus. *Journal of Refractive Surgery* 2009; 25(9):S824-S828.
92. Mihaltz K, Kovacs I, Takacs A, Nagy ZZ. Evaluation of keratometric, pachymetric, and elevation parameters of keratoconic corneas with pentacam. *Cornea* 2009; 28(9):976–80.
93. Uçakhan ÖÖ, Çetinkor V, Özkan M, Kanpolat A. Evaluation of Scheimpflug imaging parameters in subclinical keratoconus, keratoconus, and normal eyes. *Journal of Cataract & Refractive Surgery* 2011; 37(6):1116–24.
94. Bae GH, Kim JR, Kim CH, Lim DH, Chung ES, Chung T-Y. Corneal topographic and tomographic analysis of fellow eyes in unilateral keratoconus patients using Pentacam. *Am. J. Ophthalmol.* 2014; 157(1):103-109. e1.
95. Choi JA, Kim M-S. Progression of keratoconus by longitudinal assessment with corneal topography. *Invest. Ophthalmol. Vis. Sci.* 2012; 53(2):927–35.
96. Kosekahya P, Caglayan M, Koc M, Kiziltoprak H, Tekin K, Atilgan CU. Longitudinal Evaluation of the Progression of Keratoconus Using a Novel Progression Display. *Eye Contact Lens* 2019.
97. Roy AS, Dupps WJ. Patient-specific computational modeling of keratoconus progression and differential responses to collagen cross-linking. *Invest. Ophthalmol. Vis. Sci.* 2011; 52(12):9174–87.
98. Tu KL, Aslanides IM. Orbscan II anterior elevation changes following corneal collagen cross-linking treatment for keratoconus. *Journal of Refractive Surgery* 2009; 25(8):715–22.

Information which is collected as part of a standard optometric examination can be valuable for teaching and research purposes. In addition, researchers at the University of Waterloo's School of Optometry and Vision Science may also wish to contact patients about the possibility of participating in research projects.

It is for these reasons that you are being asked to give permission for persons authorized by the University of Waterloo Optometry Clinic to access identifiable personal health information contained in your University of Waterloo Optometry Clinic records and/or be contacted in future with information about research projects. Please be assured that your identity will be protected in any publication or during any public presentation of information and you are under no obligation to participate in any research projects. You may withdraw this consent at any time by informing the Clinic Administrator at 519-888-4567 extension 33582.

The decision you make with respect to access to your personal health information will not influence the eye care available to you at the School of Optometry & Vision Science.

1. I consent to allowing persons authorized by the University of Waterloo Optometry Clinic to access information from my eye examination records for teaching and/or research purposes. ☐ Yes (proceed to question 2) ☐ No (end survey)
2. I consent to allowing persons authorized by the University of Waterloo Optometry Clinic to me (by phone or email) about possible participation in research conducted at the School of Optometry and Vision Science. ☐ Yes contact ☐ No

Patient's Name: _____

Patient's Signature: _____

Telephone Number: _____

Email Address: _____

Date: _____

If patient under 16: _____

Parent's Name: _____

Parent's Signature: _____